



Available online at  
**ScienceDirect**  
www.sciencedirect.com

Elsevier Masson France  
**EM|consulte**  
www.em-consulte.com/en



Research paper

# First record of Permo-Triassic palynomorphs of the N'Condédzi sub-basin, Moatize-Minjova Coal Basin, Karoo Supergroup, Mozambique

Francesca Galasso<sup>a,b,1</sup>, Zélia Pereira<sup>c,\*</sup>, Paulo Fernandes<sup>b</sup>, Amalia Spina<sup>a</sup>, João Marques<sup>d</sup>



<sup>a</sup> Department of Physics and Geology, University of Perugia, Via Pascoli, 06123 Perugia, Italy

<sup>b</sup> Centro de Investigação Marinha e Ambiental (CIMA), Universidade do Algarve, Campus de Gambelas, 8005-139 Faro, Portugal

<sup>c</sup> Laboratório Nacional de Energia e Geologia (LNEG), Rua da Amieira, Apartado 1089, 4466-901 S. Mamede Infesta, Portugal

<sup>d</sup> Gondwana Empreendimentos e Consultorias, Limitada, Rua B, no. 233, Bairro da COOP, Caixa Postal 832, Maputo, Mozambique

## ARTICLE INFO

**Keywords:**  
Spores  
Pollen  
Lopingian  
Induan-Olenekian  
Carnian  
Karoo Palaeogeography

## ABSTRACT

Permian-Triassic ages have been identified for the first time in the Karoo Supergroup of the N'Condédzi sub-basin, Moatize-Minjova Coal Basin, Mozambique. This transition was identified in a coal exploration borehole that penetrated the Matinde and Cádzi formations. The top of the Matinde Formation is dated latest Permian (Lopingian), and the Cádzi Formation is attributed to Triassic based on palynostratigraphy. The Lopingian age is established by the identification of three palyno-assemblages: Assemblage L1 based on the first occurrence (FO) of *Guttulapollenites* pollen, Assemblage L2 is marked by the FO of *Thymospora pseudothiessenii*, and Assemblage L3 is defined by the FO of *Osmundacidites senectus*. Triassic palynomorphs were identified for the first time in Mozambique (Karoo basins). The data allowed the identification of three assemblages: Assemblage T1 defined by the FO of *Densoisporites nejburgii* of Induan age, Assemblage T2 is marked by the FO of *Platysaccus queenslandi* and assigned to the Olenekian age, and Assemblage T3 is defined by the FO of *Samaropollenites speciosus* and *Enzonalsporites vigens*, indicating a Carnian age. No Middle Triassic rocks were identified, and the early Triassic sediments are overlain by sedimentary rocks of Carnian age, a hiatus that may correspond to an important tectonic event with uplift and erosion. This tectonic event is also suggested by the occurrence of common reworked Permian palynomorphs in the Carnian sedimentary rocks. These new data constrain the age of the Karoo Supergroup formations of Mozambique and contribute to improve the palaeoecological, palaeoclimatic evolution, and the palaeogeographic position of the Karoo Mozambique basins within the Gondwana supercontinent.

© 2019 Elsevier Masson SAS. All rights reserved.

## 1. Introduction

In the last decade, the increase in the exploration and exploitation of coal in the Mozambique Karoo basins is documented especially in the region surrounding Tete city, in the Province of Tete (Fig. 1). This growth was due, in part, to an effort initiated several years earlier by the Mozambican Geological Survey (Direcção Nacional de Geologia) that in partnership with other countries geological surveys revised the geology of the entire country, leading to the publication of a new series of geological maps (GTK Consortium, 2006; Norconsult Consortium, 2007). Regarding the geology of the

Karoo sequences, new lithostratigraphic units were proposed (GTK Consortium, 2006; Paulino et al., 2010). However, these new stratigraphic studies were not complemented, from the beginning, with scientific works directed to exploration decisions and associated to reduce risks related to this activity. For example, until the present, very few paleontological, palynological, and palaeoecological studies that ascertain the age and the depositional conditions of the coal-bearing basins have been published. Specifically, regarding coal exploration, this significant mapping effort led to the definition and concession of new areas for exploration that were followed by intensive drilling campaigns. Thus, boreholes made recently available by several exploration companies are supporting the completion of numerous studies in the Moatize-Minjova Coal Basin (MMCB) (Fig. 1) including palynostratigraphy (Pereira et al., 2014; Lopes et al., 2014; Pereira et al., 2016; Götz et al., 2018), thermal history (Fernandes et al., 2015; Galasso et al., 2019), Permian climatic

\* Corresponding author.

E-mail address: zelia.pereira@lneg.pt (Z. Pereira).

<sup>1</sup> Currently at University of Zurich.

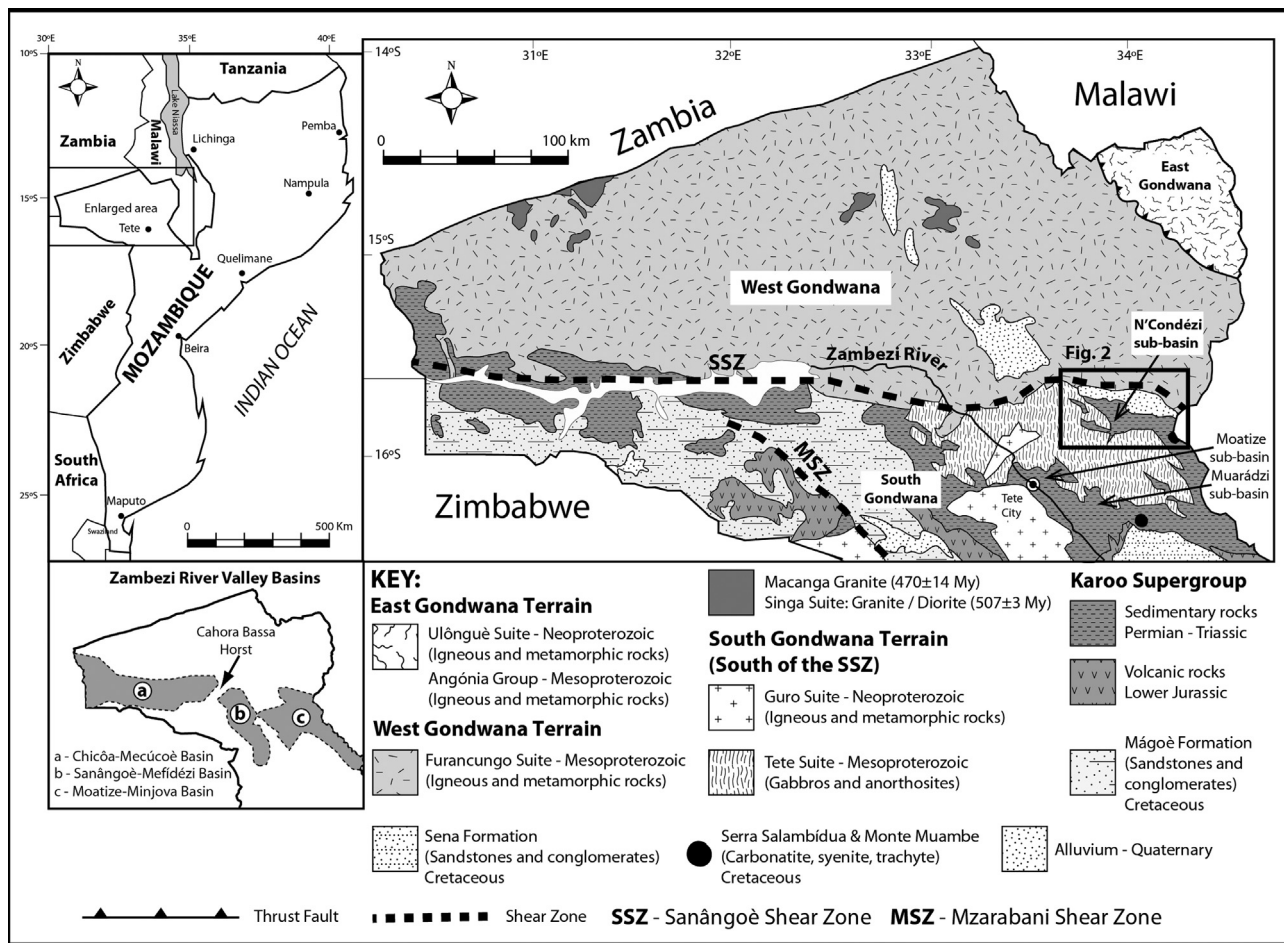


**Fig. 1.** Simplified geology of the Tete Province, Mozambique, with the location of Karoo basins of the Zambezi river valley and the N'Condédzi, Moatize and Muarádzi sub-basins.

Adapted from *Geological Map of Mozambique*, Direcção Nacional de Geologia, Maputo (2006).

changes (Götz et al., 2017), the tectonostratigraphy (Bicca et al., 2017) and sediment provenance (Bicca et al., 2018). The present work deals with the palynostratigraphy of the formations positioned at the top of the Karoo Supergroup stratigraphic succession of Mozambique, aiming to date these formations, and to contribute to a better understanding and characterise the palaeoecological and palaeoclimatic features recorded in these deposits. With this study, we will aim to improve the knowledge on the palaeogeographic position of these basins within the Gondwana supercontinent and ultimately contribute to coal seam identification and correlation required in future coal exploration programmes.

## 2. Geological setting of the N'Condédzi sub-basin

The N'Condédzi sub-basin is one of the several sub-basins that form the main MNCB. In turn, the MNCB is one of the three main basins located along the Zambezi river valley in the province of Tete (Lächelt, 2004; GTK Consortium, 2006) (Fig. 1). The MNCB is the best studied of all the Karoo basins in Mozambique, mainly due to the presence of abundant coal seams, which are currently being exploited in two mines (Vale Moatize and ICLV Benga mines). The development of Karoo basins in the province of Tete is related to the brittle reactivation of high strain shear zone (e.g., the Sanângoê and Mzarabani shear zones) of the Zambezi Belt, formed during the Pan-African Orogeny (620–530 Ma) (Carvalho, 1977; Afonso, 1984; Pinna et al., 1993; Jamal, 2005; GTK Consortium, 2006; Norconsult Consortium, 2007; Grantham et al., 2008; Viola et al., 2008).

The stratigraphic succession of the MNCB consists of four clastic formations, which are from base to top, Vúzi, Moatize, Matinde, and Cádzi formations. From these lithostratigraphic units, the Moatize Formation in its type area (around Moatize town) has six main coal seams interbedded with sandstones and mudstones. Parts of these stratigraphic units were recognized in the N'Condédzi sub-basin (Lakshminarayana, 2015), whose general geology is described below; however, a detailed description of the geology and lithostratigraphy of the MNCB can be found in publications such as Lächelt (2004), GTK Consortium (2006), Vasconcelos (2013), Fernandes et al. (2015) and Pereira et al. (2016).

A comprehensive work on the N'Condédzi sub-basin was published by Lakshminarayana (2015). Although this work is mainly focused on several aspects of coal geology and exploration, it also provides new information about the stratigraphic succession in this area. The N'Condédzi sub-basin is located ca. 50 km to NE of the Tete city (Fig. 1). Its northern boundary corresponds to the Mwanza Fault (Fig. 2), a brittle structure formed by the reactivation of the Sanângoê Shear Zone (SSZ) during the early(?) Permian, and related to the initial tectonic phases of this sub-basin development. The Mwanza Fault is a prominent geomorphologic feature at the northern boundary of this sub-basin, separating the granites and gneisses of the Mesoproterozoic Furancungo Suite and the flat region of the hanging wall fault block that corresponds to the Karoo sedimentary rocks (Fig. 2). According to Lakshminarayana (2015), the throw of the Mwanza Fault is more than 700 m towards the south, but Galasso et al. (2019) estimates that the throw of

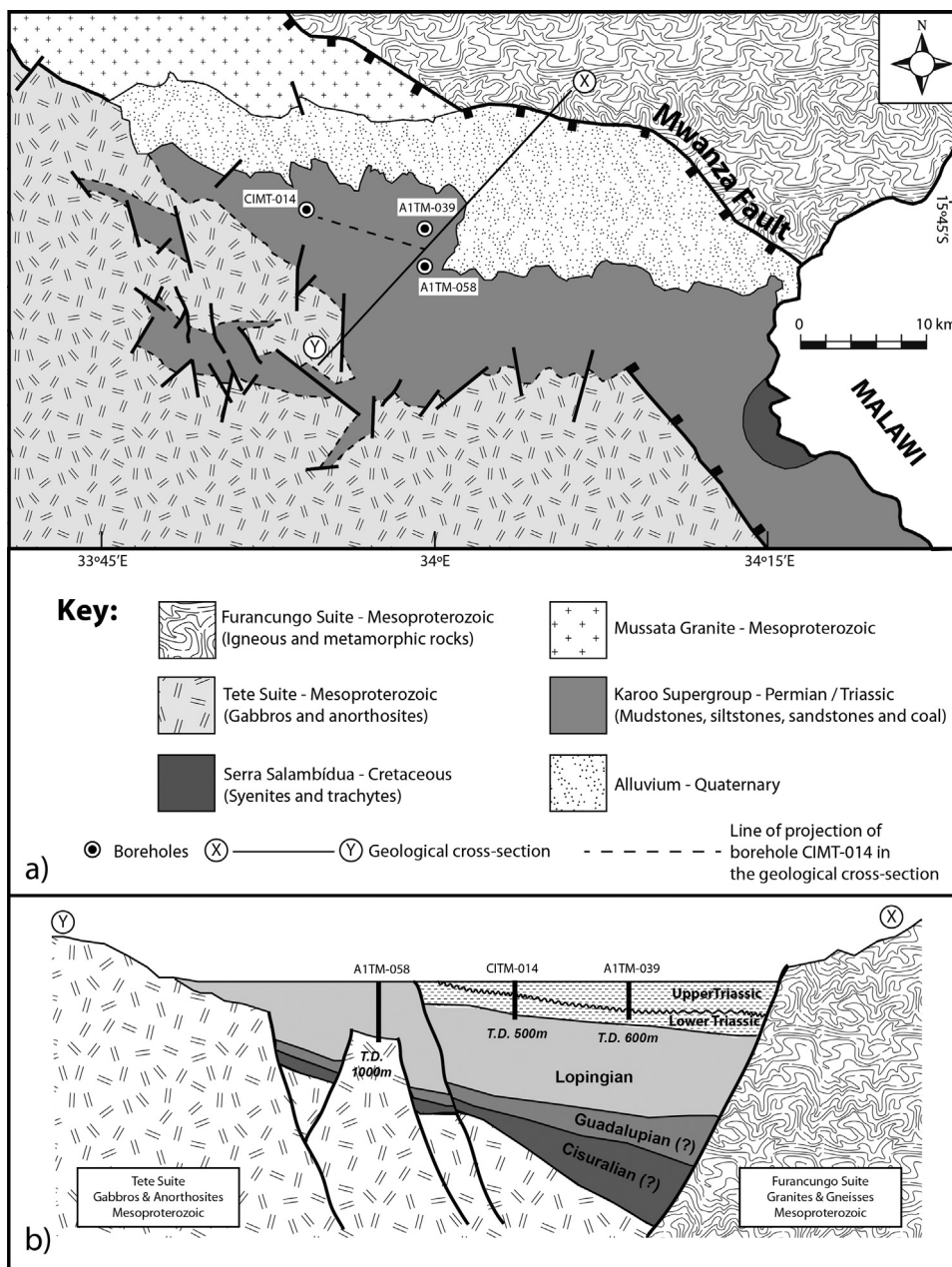


**Fig. 2.** a: detailed geological map of the N'Condédzi sub-basin, showing the location of the boreholes studied; b: interpretative geological cross-section of the N'Condédzi sub-basin with the location of the boreholes studied, showing also the age of the stratigraphic successions penetrated by the three boreholes. The wavy line in the cross-section corresponds to the hiatus between the lower and upper Triassic rocks. Geological cross-section not at scale. Adapted from Geological Map of Mozambique, Sheet No. 1533/1534, Cazula/Zôbuê, Geological Series 1/250,000, Direcção Nacional de Geologia, Maputo (2006).

this fault is more than 1000 m towards the same direction, due to the presence of a combined Lopingian to Middle Triassic succession with a thickness of ca. 1500 m. In the southern margin of this sub-basin, Karoo sedimentary rocks rest either unconformably over the Mesoproterozoic gabbros-anorthosites of the Tete Suite or are faulted against the later lithologies (Fig. 2). Different ages of the Karoo sedimentary rocks positioned immediately above the crystalline basement rocks, located in different positions of this basin (Galasso et al., 2019 and in present work), suggest that the Karoo sediments progressively overstepped the gentle tilted basement rocks towards South-Southwest (today's coordinates).

According to Lakshminarayana (2015), the stratigraphic succession of the N'Condédzi sub-basin starts, at the base, by the Vúzi Formation, which consists of clast to matrix-supported conglomerates and sandstones arranged into fining-upward cycles

deposited in periglacial environments. The thickness of this formation varies from 60 to 140 m. The Vúzi Formation passes upward to the 'Transitional Assemblage', a new informal lithostratigraphic unit defined by Lakshminarayana (2015). The latter unit consists of conglomerates, sandstones, mudstones, and cm-thick coal beds organized vertically into several fining-upward cycles, each cycle with a thickness of 3 to 5 m, in an overall thickness of ca. 70 m. This informal unit was deposited in the proximal areas of a major alluvial fan, characterise by plain-coal swamps in the distal parts of the fan. Above this unit, lays conformably the Moatize Formation, which is divided into two different lithofacies groups: a dominant sandstone lithofacies, consisting of sandstones interbedded with siltstones and mudstones, and the coal-carbonaceous mudstones lithofacies (Lakshminarayana, 2015). The latter consists of cyclic coal beds interbedded with carbonaceous mudstones and

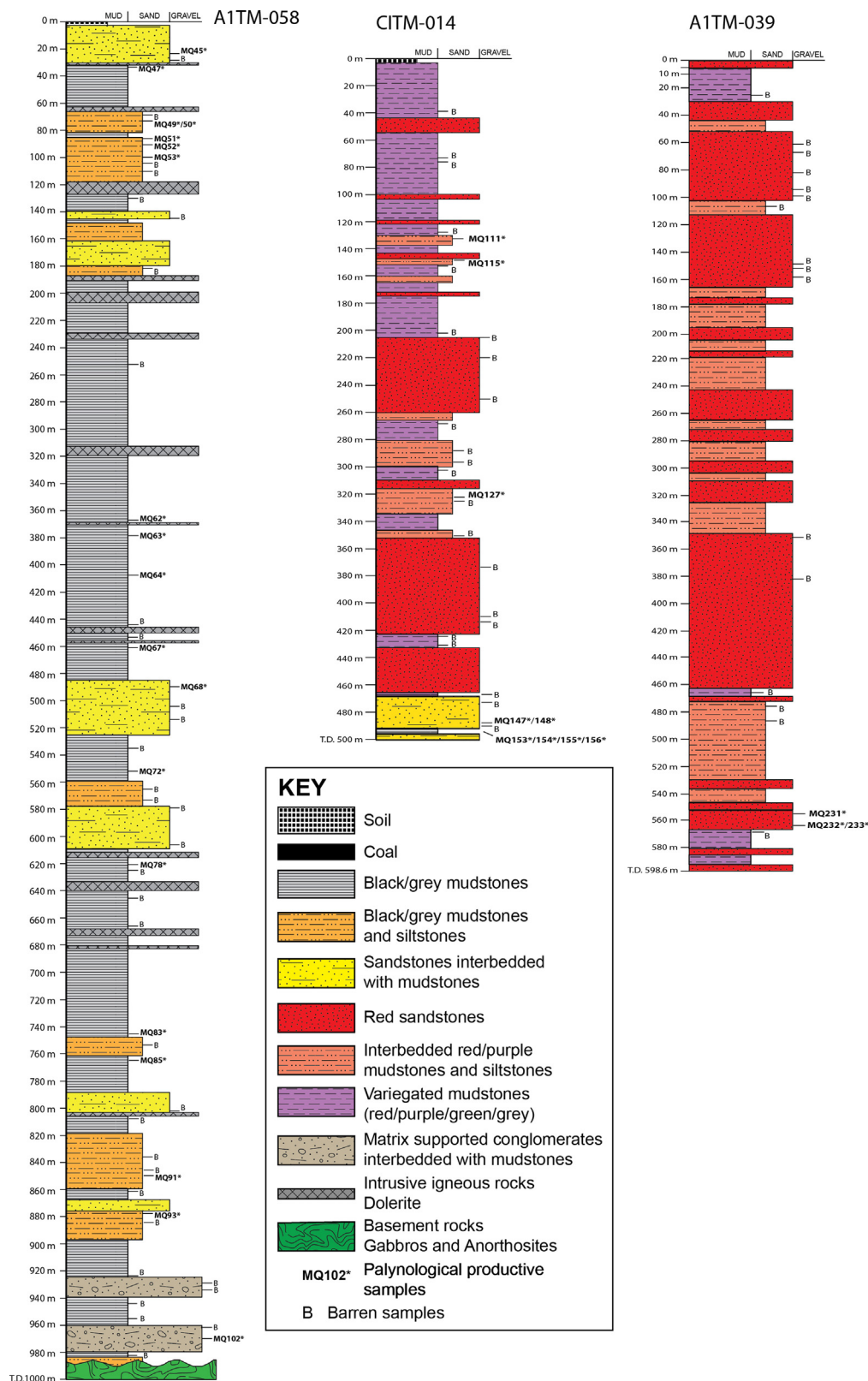


Fig. 3. Lithological logs of boreholes A1TM-058, C1TM-014 and A1TM-039 with the position of the studied palynological samples.

siltstones, comprising the so-called barcode coal seams, constituting almost two-thirds of the overall thickness of the Moatize Formation. The thickness of Moatize Formation is more than 400 m in this sub-basin. The main Coal Seams or ‘Carbonaceous Complexes’ of the Moatize Formation, defined in the type area of the Moatize

(Benga) sub-basin, are recognized in the N’Condédzi sub-basin (Lakshminarayana, 2015). There are, however, some differences between the stratigraphy of the two sub-basins: in the N’Condédzi sub-basin, the *Sousa Pinto Coal Seam* occurs within the ‘*Transitional Assemblage*’, and not at the base of the Moatize Formation; the

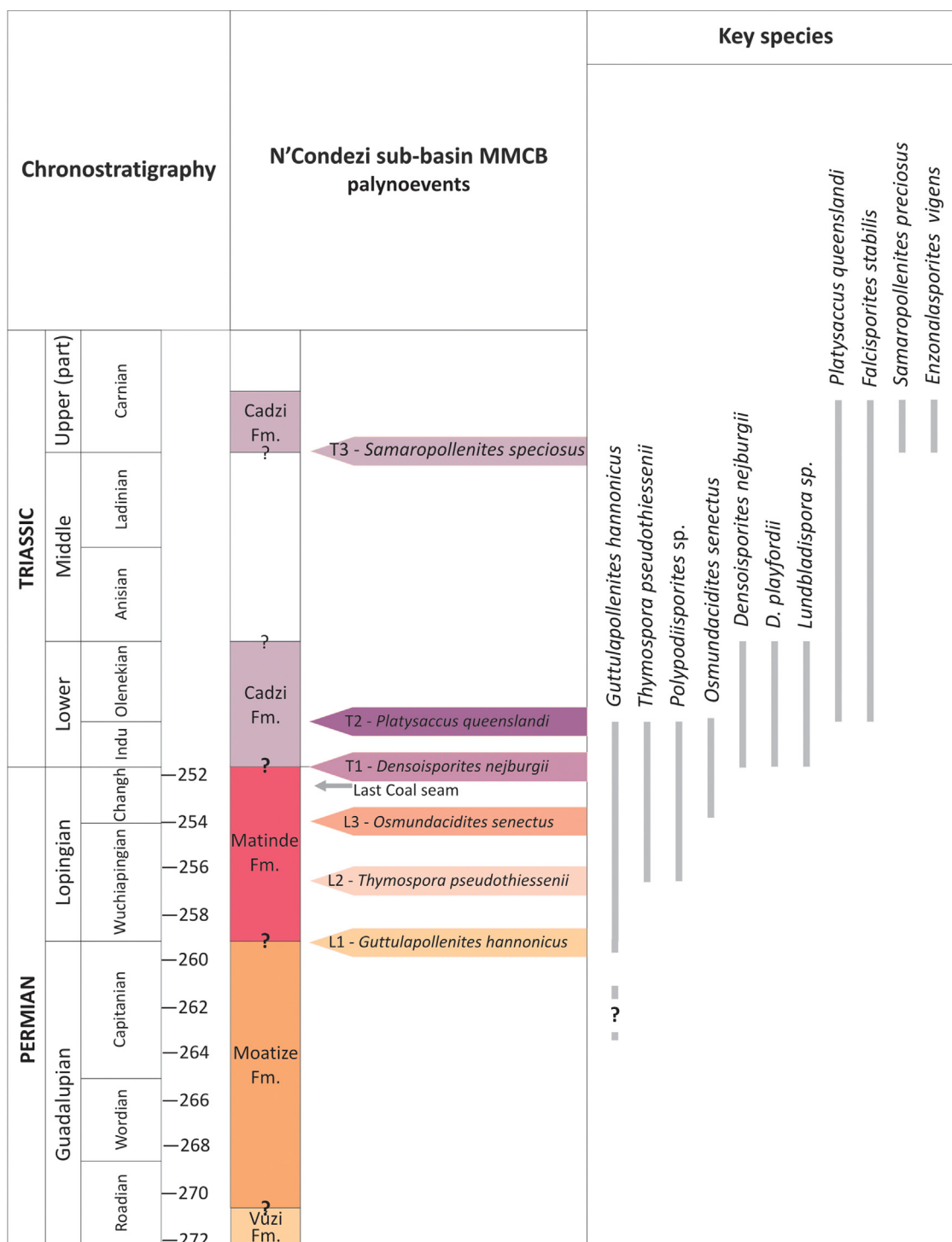


Fig. 4. Main palynological events and key species recovered in the N'Condezi sub-basin, Moatize-Minjova Basin, Mozambique.

*Grande Falésia* and *André Coal Seams* are better developed in the N'Condezi sub-basin, especially the *Grande Falésia* whose thickness varies between 110 and 250 m, in clear contrast with the 12 m thickness recognized for this coal seam in the Moatize sub-basin (Lächelt, 2004).

The Matinde Formation conformably overlays the Moatize Formation and comprises conglomerates and thick beds of coarse-to-medium-grained sandstones, with rare interbedded mudstones. The thickness of the Matinde Formation in this sub-basin is unknown. Palaeocurrents measured in cross-bedded sandstones of the Matinde Formation show a predominant ESE direction

(Lakshminarayana, 2015). The stratigraphic succession terminates with the Cádzi Formation that consists of conglomerates, red coarse-to-medium-grained sandstones, interbedded with red to green mudstones. Dolerite sills related to the Lower Jurassic Karoo-Ferrar Large Igneous Province (Duncan et al., 1997) are found intruded, especially in the Moatize Formation.

Due to the absence of any biostratigraphic information, Lakshminarayana (2015) correlated the Vúzi Formation with the late Pennsylvanian–early Cisuralian Dwyka Group of the Main Karoo Basin of South Africa and the Moatize and Matinde formations with the Cisuralian–early Lopingian Ecça Group.

### 3. Material and methods

Ninety-nine core samples were collected for a palynostratigraphic study from three coal exploration boreholes (A1TM-058, CIMT-014 and A1TM-039) drilled in the N'Condédzi sub-basin (Figs. 2 and 3). Thirty-one samples proved productive containing moderately preserved and diversified palynomorphs. A minimum of 200 palynomorphs were counted per slide (Tables 1–3). The following adjectives were used to describe the different palynomorphs identified: Abundant (>50%), Common (10–50%), and Rare (<10%).

The palynological samples were treated with standard palynological laboratory procedures to extract and concentrate the organic matter. The organic residues were oxidized using fuming nitric acid for approximately 1 minute (Wood et al., 1996; Riding and Warny, 2008). The slides were examined under transmitted light, with a BX40 Olympus microscope equipped with an Olympus C5050 digital camera and Qualitative spore fluorescence colours was undertaken in the University of the Algarve using an Olympus BX51 microscope equipped with a metal halide lamp fluorescence unit (XCite Series 120Q) and with a violet and Blue +12 filter block that generates a wavelength band of 390–490 nm. This system was allowed to stabilize for 5 minutes before any observation of the fluorescence of palynomorphs was attempted. All samples, residues and slides are held both in the University of the Algarve, Portugal, and in the Collection of the Geological Survey of Portugal, LNEG, S. Mamede de Infesta. Selected palynomorphs are illustrated in Plates 1–5.

### 4. Borehole lithostratigraphic description

#### 4.1. Borehole A1TM-058

This borehole attained a total depth of 1000 m and penetrated, at its base, a 4 m sequence of basement rocks (gabbro-anorthosites) belonging to the Mesoproterozoic Tete Suite (Fig. 3). The basement rocks are unconformably overlain by an 8 m thick sequence consisting of red siltstones interbedded with red mudstones that pass upwards to black carbonaceous mudstones beds. The 980 m to 930 m depth interval consists of two sections of clast to matrix-supported conglomerates interbedded with black mudstones and black carbonaceous mudstones. The latter interval is followed by a succession of approximately 180 m thick of cyclic sandstones/siltstones beds interbedded with black mudstones. Most of the succession above 750 m, and to 190 m depth, comprises black carbonaceous mudstones, black mudstones, siltstones and coal beds, with the coarser lithologies (sandstones) concentrated between 610 m to 490 m depth. This thick interval is also characterised by the occurrence of several intrusive dolerite sills. From 190 m depth to the top of the borehole, the succession consists of coarse- to medium-grained sandstones intercalated with siltstones, carbonaceous mudstones and thin coal beds.

#### 4.2. Borehole CIMT-014

The borehole succession consists mainly of red clastic lithologies, which are in clear contrast with the succession of the previous borehole, denoting a marked change in the depositional and palaeoenvironmental settings. This borehole has a total depth of 500 m (Fig. 3), and the succession from total depth to ca. 489 m is dominated by intercalations of black carbonaceous mudstones, siltstones, and fine-grained sandstones beds. The interval from 484.5 m to 463 m depth consists of grey siltstones interbedded with fine-grained grey sandstones that are followed upwards by a 4.5 m thick bed of clast-supported conglomerates interbedded with two

centimetric thick grey mudstones beds. From ca. 463 m to 350 m depth, there is a second prominent sandstone-dominated interval consisting of red to purple conglomerates, coarse- to medium-grained sandstones interbedded with rare red-brown mudstones and siltstones. The succession between 350 m and 260 m depth consists of fine-grained lithologies, red mudstones and siltstones with few medium-grained sandstone beds. A prominent coarse- to medium-grained sandstone section with rare grey mudstone lenses characterises the following 50 m interval, which ends at 210 m depth. Lastly, from 210 m depth to the top of the borehole, the succession is dominated by red-brown mudstones interbedded with thin beds of brown siltstones, medium-grained red-yellow sandstones and rare lenses of grey mudstones.

#### 4.3. Borehole A1TM-039

As borehole CIMT-014, this borehole penetrated approximately 600 m of mainly red clastic sedimentary beds (Fig. 3). However, borehole A1TM-039 is richer in coarse-grained clastic sedimentary rocks than borehole CIMT-014. From total depth to ca. 564 m depth, the succession consists of grey-black mudstones interbedded with yellow buff medium-grained sandstones. From 564 m to 470 m depth, the succession consists of red-brown siltstones interbedded with red mudstone beds and few red sandstones levels. Following upwards, the interval from 470 m to 350 m depth is dominated by thick coarse- to medium-grained red-pink sandstone beds. Finally, from 350 m to the top of the borehole, the succession comprises thick conglomerate beds and coarse- to medium-grained sandstones that are intercalated with less common red-brown siltstones and mudstones beds.

### 5. Palynological results

The quantitative and qualitative distribution of the palynomorph assemblages presented is based on the relative abundance of the taxa and on the FO of particular taxa. Three assemblages of Lopingian age (L1 to L3), also identified in the stratigraphic succession of the Muarádzi sub-basin of the MMB (Pereira et al., 2019), and three assemblages assigned to the Triassic (T1 to T3) are described in this work (Tables 1–3).

In stratigraphic order, the palynomorph assemblages are as follows.

#### 5.1. Assemblage L1

This assemblage is characterised by a clear dominance of gymnosperms taeniate bisaccate pollen (*Protohaploxylinus* spp. and *Striatopodocarpites* spp.) and non-taeniate pollen (*Alisporites* spp.). Typical taxa are *Alisporites* spp. (*A. plicatus*, *A. potoniei*, *A. ovatus*), *Protohaploxylinus* spp. (e.g., *P. amplus*, *P. diagonalis*, *P. goraiensis*, *P. hartii* and *P. limpidus*) and *Striatopodocarpites* spp., as well as rare to common *Cycadopites cymbatus*, *Lueckisporites virkkiae*, *Platysaccus* sp. and *Vittatina* spp. Common to abundant *Guttulapollenites hannonicus* and *Weylandites lucifer*, as well as rare to common monosaccate pollen assigned to the taxa *Cannanoropolis* sp. are also present. Spores are rare to common and include *Apiculatisporis* sp., *Baculatisporites* sp., *Brevitriletes cornutus*, *Brevitriletes* sp., *Calamospora* spp., *Cyclogranisporites* sp., *Fabaspores* sp., *Horriditriletes* spp., *Laevigatisporites* spp., *Leiotriletes* sp. and rare *Microbaculispora* sp., *Procoronaspora spinosa*, *Verrucosisporites* sp. and *Verrucosisporites andersonii* (Table 1).

Occurrence: Borehole A1TM-058, sample interval MQ102 to MQ85.

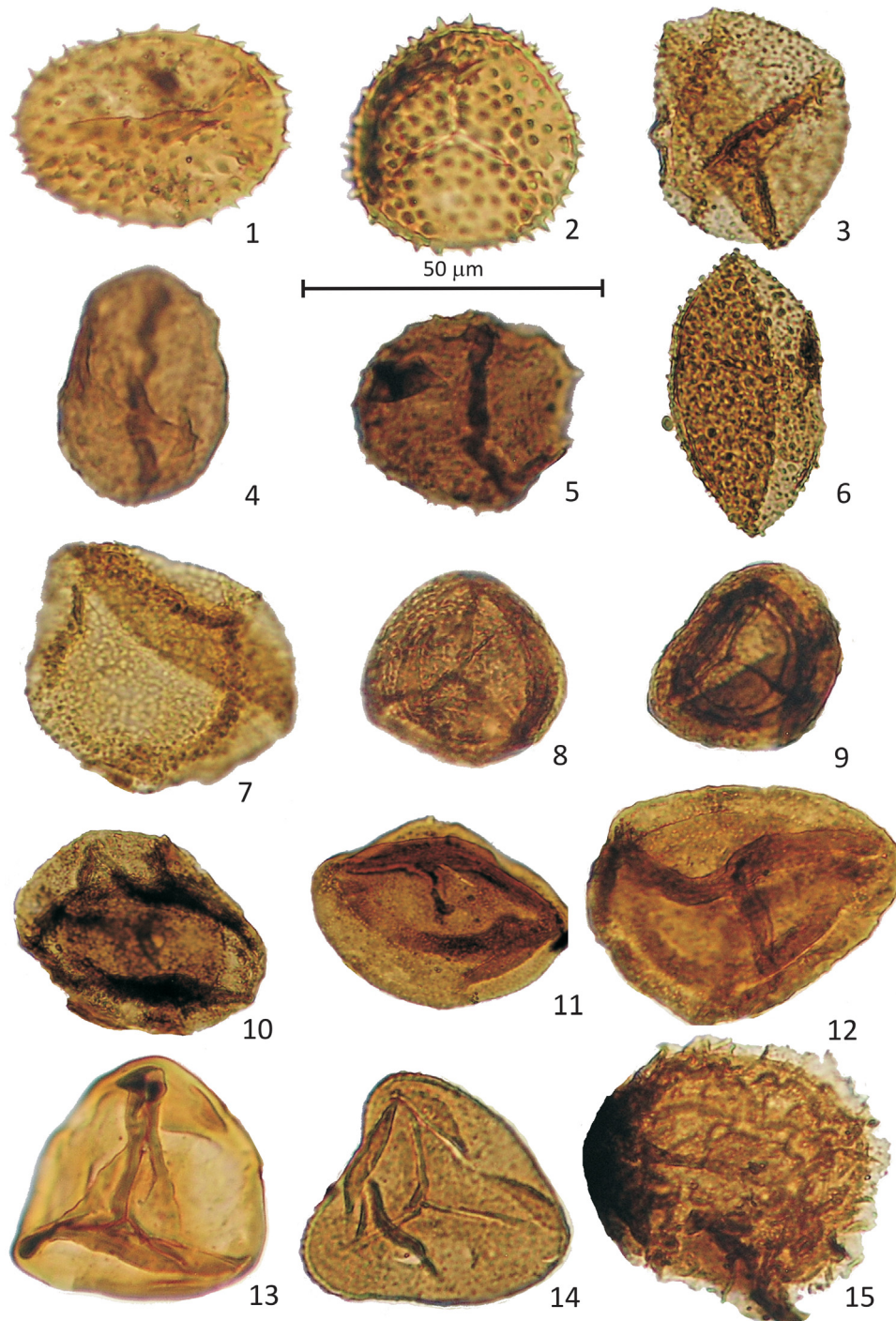


**Plate 1.** Selected palynomorph specimens from the N'Condédzi sub-basin, MNCB, Mozambique. Plate captions give the taxonomic name of the figured specimen, followed by borehole reference, sample number, slide number and microscope coordinates (MC). Scale bars: 50 µm. 1. *Anapiculatisporites spiniger* (Leschik) Reinhardt/*Carnisporites anteriscus* Morbey, 1975, Borehole CIMT-014, Sample MQ111, Slide 1a-16, MC1410-38, EF X42/3; 2. *Anapiculatisporites spiniger* (Leschik) Reinhardt/*Carnisporites anteriscus* Morbey, 1975, Borehole CIMT-014, Sample MQ 111, Slide 4-19, MC1338-135, EF N34/4; 3. *Baculatisporites bharadwaji* Hart, 1963, Borehole CIMT-014, Sample MQ 148, Slide 1b-9, MC1375-75, EFT38; 4. *Aratrisporites* sp., Borehole A1TM-039, Sample MQ233, Slide 2-47, MC 1440-55, EF V45; 5. *Aratrisporites* sp., Borehole A1TM-039, Sample MQ 233, Slide 2-146, MC 1405-105, EF Q41/4; 6. *Baculatisporites* sp., Borehole CIMT-014, Sample MQ 147, Slide 1b-18, MC 1285-50, EF W29; 7. *Cyclogranisporites* sp., Reworked, Borehole CIMT-014, Sample MQ 111, Slide 2a-126, MC1375-65, EF U38/4; 8. *Densoisporites complicatus* Balme, 1970, Borehole CIMT-014, Sample MQ 111, Slide 4-55, MC 1120-78, EF S12/3; 9. *Densoisporites playfordii* (Balme, 1963) Balme, 1970, Borehole CIMT-014, Sample MQ 111, Slide 5-120, MC 1245-255, EF A25/2; 10. *Densoisporites neburgii* (Schulz, 1964) Balme, 1970, Borehole CIMT-014, Sample MQ 147, Slide 1a-79, MC 1430-195, EFG44; 11. *Densoisporites playfordii* (Balme, 1963) Balme, 1970, Borehole CIMT-014, Sample MQ 147, Slide 5-149, MC 1270-75, EFT27; 12. *Densoisporites playfordii* (Balme, 1963) Balme, 1970, Borehole CIMT-014, Sample MQ 111, Slide 4-42, MC 1125-75, EF T12/2; 13. cf. *Dictyophyllidites* sp., Borehole CIMT-014, Sample MQ 111, Slide 4-2, MC 1245-95, EF R25; 14. *Lophotriletes novicus* Singh, 1964, Borehole CIMT-014, Sample MQ 147, Slide 5-3, MC 1510-65, EF R25/4; 15. *Kraeuselisporites* sp., Borehole CIMT-014, Sample MQ 111, Slide 2b-34, MC 1310-140, EF M31/4.

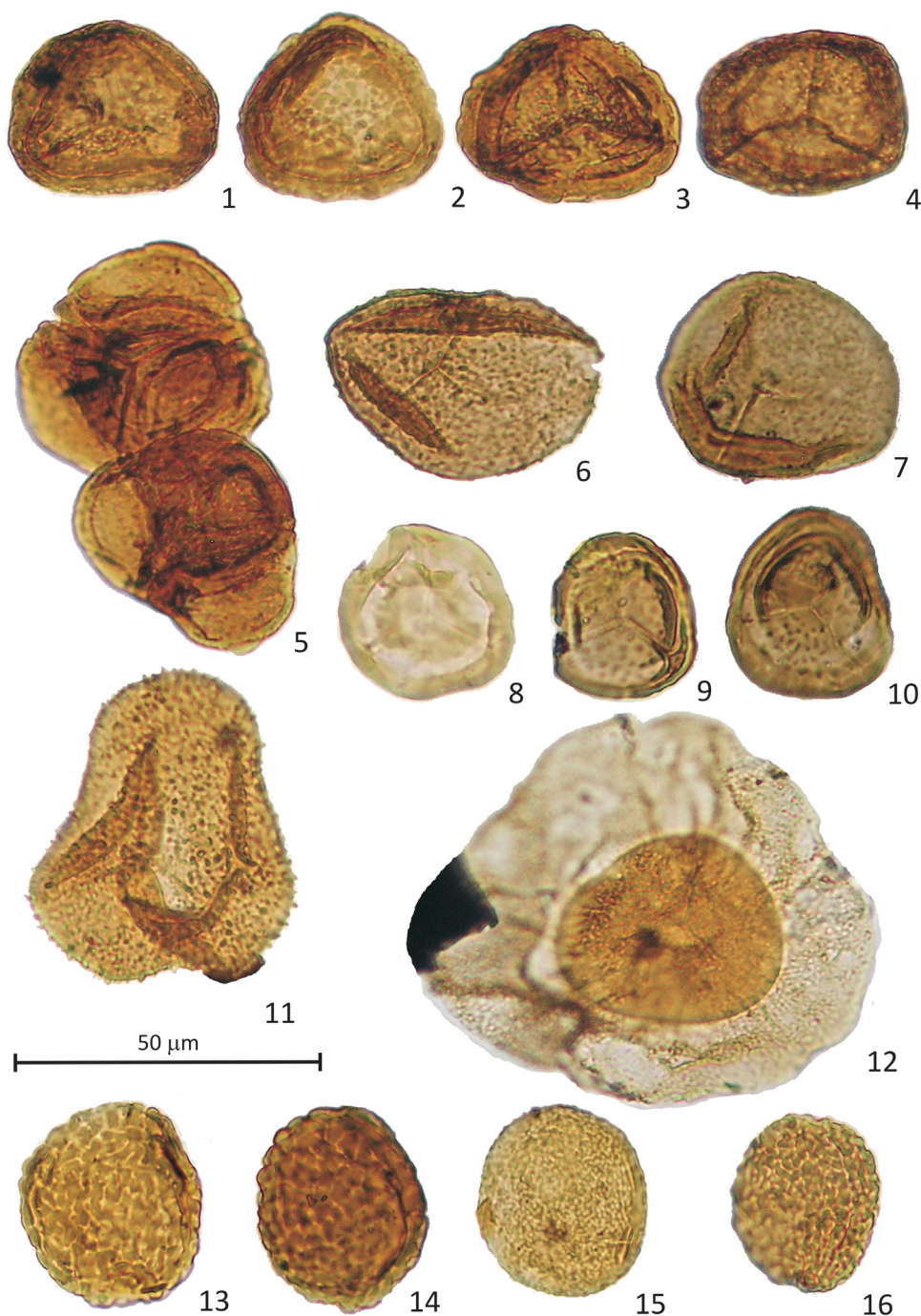


**Plate 2.** Selected palynomorph specimens from the N'Condédzi sub-basin, MMCB, Mozambique. Plate captions give the taxonomic name of the figured specimen, followed by borehole reference, sample number, slide number and microscope coordinates (MC). Scale bars: 50 μm. 1. *Lundbladispora brevicula* Balme, 1963, Borehole CIMT-014, Sample MQ 111, Slide 4a-15, MC 1325-110, EF P34; 2. *Lundbladispora brevicula* Balme, 1963, Borehole CIMT-014, Sample MQ 111, Slide 4a-29, MC1350-125, EF P33/4; 3. *Lundbladispora* sp. Borehole CIMT-014, Sample MQ 111, Slide 3-125, MC 1235-105, EF Q24; 4. *Lundbladispora* sp. Borehole CIMT-014, Sample MQ 111, Slide 4a-45, MC 1125-75, EF S13/4; 5. *Lundbladispora* tetrad, Borehole CIMT-014, Sample MQ 111, Slide 3-119, MC 1132-160, EF K13/4; 6. *Osmundacidites senectus* Balme, 1970, Reworked, Borehole CIMT-014, Sample MQ 111, Slide 2a-73, MC1385-95, EF R39/4; 7. *Osmundacidites senectus* Balme, 1970, Reworked, Borehole A1TM-039, Sample MQ 233; Slide 2-137, MC1300-60, EF V30/2; 8. *Nevesisporites fossulatus* Balme, 1970, Borehole CIMT-014, Sample MQ 111, Slide 3-122, MC1055-110, EF P5/4; 9. *Limatulasporites limatulus* (Playford, 1965) Helby and Foster, 1979, Borehole A1TM-039, Sample MQ 232, Slide 2b-148, MC 1405-105, EF Q41/2; 10. *Limatulasporites limatulus* (Playford, 1965) Helby and Foster, 1979, Borehole CIMT-014, Sample MQ 111, Slide 3-124, MC1235-105, EF P24/4; 11. *Microbaculatisporites* sp., Reworked, Borehole CIMT-014, Sample MQ 111, Slide 4-48, MC1125-75, EF S13; 12. *Playfordiaspora cancellosa* (Playford and Dettmann) Maheshwari and Banerji, 1975, Borehole CIMT-014, Sample MQ 111, Slide 3-105, MC 1120-115, EF P12/2; 13. *Polypodiisporites* sp. sensu Balme, 1970, Borehole CIMT-014, Sample MQ 148, Slide 1a-92, MC1445-100, EF R25/2; 14. *Polypodiisporites* sp. sensu Balme, 1970, Reworked, Borehole A1TM-039, Sample MQ 232, Slide 2b-83, MC 1450-172, EF J46/4; 15. *Thymospora pseudothiessenii* (Kosanke) Wilson and Venkatachala, 1963, Borehole CIMT-014, Sample MQ 148, Slide 1a-5, MC 1380-135, EF 39/3; 16. *Thymospora pseudothiessenii* (Kosanke) Wilson and Venkatachala, 1963, Reworked, Borehole A1TM-039, Sample MQ 231, Slide 3b-29, MC 1135-190, EF H14/1.

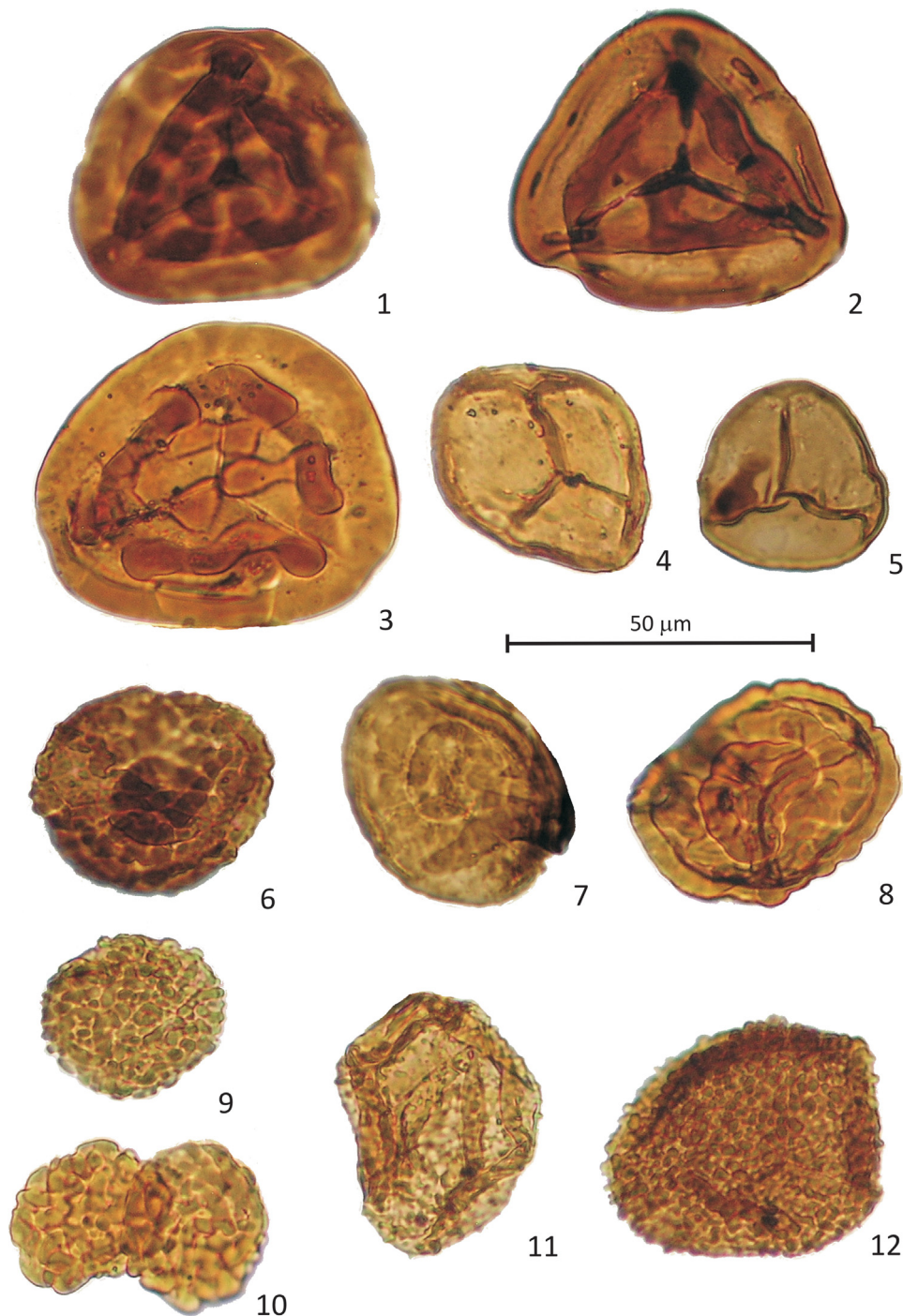


**Plate 3.** Selected palynomorph specimens from the N'Condédzi sub-basin, MNCB, Mozambique. Plate captions give the taxonomic name of the figured specimen, followed by borehole reference, sample number, slide number and microscope coordinates (MC). Scale bars: 50 μm. 1. *Striatella seebergensis* Madler, 1964, Borehole CIMT-014, Sample MQ 111, Slide 2a-36, MC1445-90, EF S46; 2. *Striatella* sp., Borehole CIMT-014, Sample MQ 111, Slide 2a-129, MC1350-100, EF 36/1; 3. *Striatella seebergensis* Madler, 1964, Borehole CIMT-014, Sample MQ 111, Slide 4a-11, MC1235-85, EF S24/4; 4. *Retusotriletes* sp., Borehole CIMT-014, Sample MQ 111, Slide 1a-9, MC1422-80, EF T43/2; 5. *Stereisporites* sp., Borehole CIMT-014, Sample MQ 111, Slide 3a-98, MC1085-70, EF U8; 6. *Taurocusporites* sp., Borehole CIMT-014, Sample MQ 111, Slide 1a-152, MC1405-195, EF F42/3; 7. *Taurocusporites* sp., Borehole CIMT-014, Sample MQ 111, Slide 2a-165, MC1325-175, EF T33; 8. *Taurocusporites* sp., Borehole CIMT-014, Sample MQ 111, Slide 4-61, MC1170-190, EF 17/4; 9. *Leptolepidites* sp., Borehole A1TM-039, Sample MQ 233, Slide 2-36, MC1440-65, EF V45/1; 10. *Leptolepidites* sp., Borehole A1TM-039, Sample MQ 233, Slide 2-84, MC1398-155, EF L40/4; 11. *Verrucosiporites andersonii* Backhouse, 1988, Reworked, Borehole CIMT-014, Sample MQ 111, Slide 1a-68, MC1415-150, EF L42/4; 12. *Verrucosiporites narnianus* Balme, 1970, Borehole CIMT-014, Sample MQ 111, Slide 2a-172, MC1305-75, EF T31.

### 5.2. Assemblage L2

The assemblage contains abundant *Alisporites* spp. (including *A. plicatus*, *A. potonieii* and *A. ovatus*), *Protohaploxylinus* spp. (e.g., *Protohaploxylinus amplus*, *P. goraiensis* and *P. limpidus*) and *Striatopodocarpites* spp., together with rare to common *Vittatina* sp. and

*Weylandites lucifer*. Other rare to common pollen taxa occurring in this assemblage are *Cycadopites* sp., *Lueckisporites virkkiae* and *Gnetaceapollenites sinuosus*, in addition to common *Guttulapollenites hannonicus* and *Platysaccus* sp.

The spores increase in abundance: taxa such as *Brevitriletes* sp. *Baculatisporites bharadwaji*, *Baculatisporites* sp., *Calamospora*

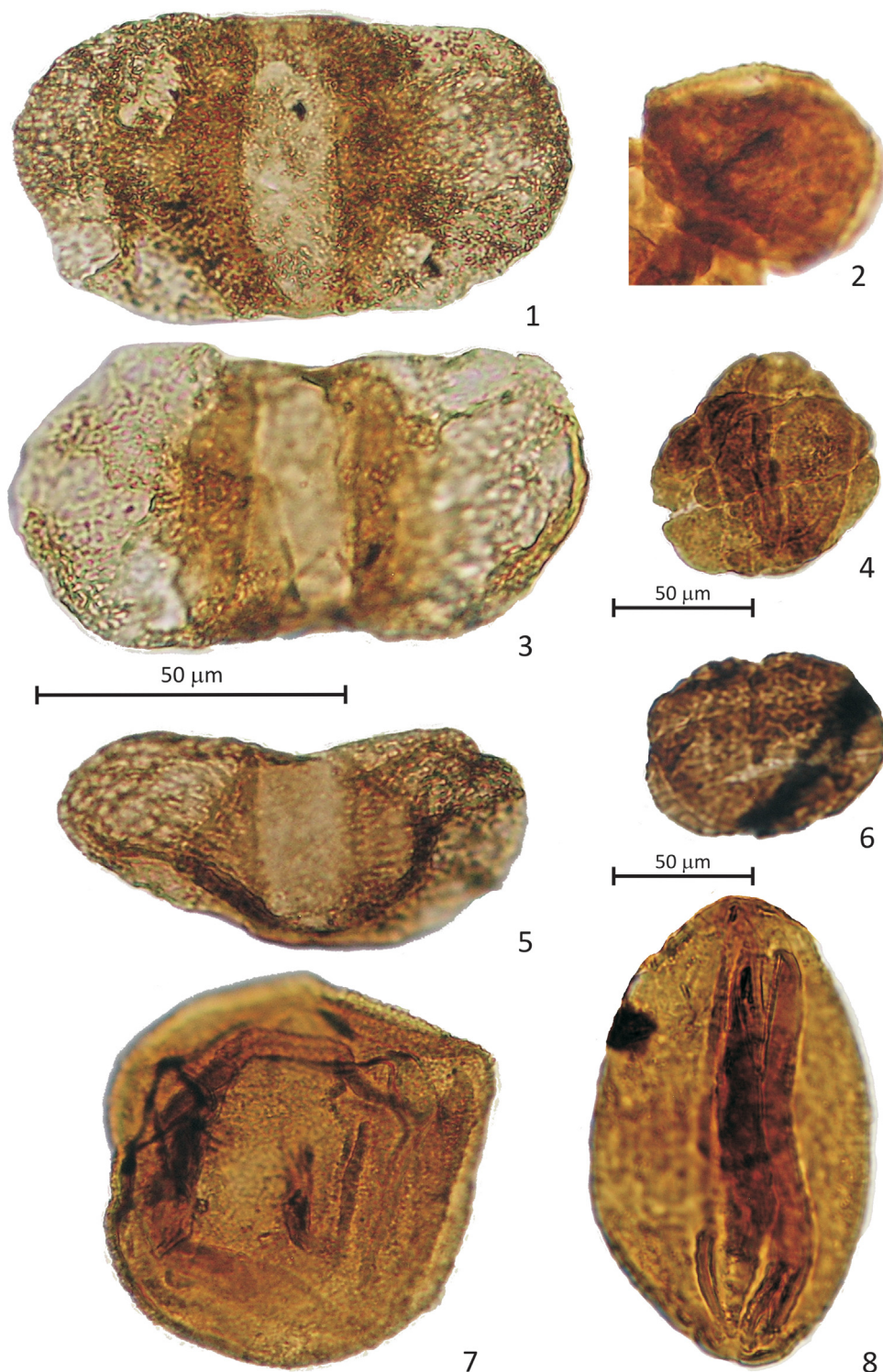


**Plate 4.** Selected palynomorph specimens from the N'Condédzi sub-basin, MNCB, Mozambique. Plate captions give the taxonomic name of the figured specimen, followed by borehole reference, sample number, slide number and microscope coordinates (MC). Scale bars: 50 μm. 1. *Alisporites parvus* de Jersey, 1962, Borehole CIMT-014, Sample MQ 111, Slide 1a-30, MC1415-55, EF 2V4; 2. *Enzonalaspores vigenis* Leschik, 1955, Borehole A1TM-039, Sample MQ 232, Slide 1-1, MC1225-55, EF V26; 3. *Alisporites parvus* de Jersey 1962, Borehole A1TM-039, Sample MQ 232, Slide 2b-23, MC1225-42, EF X23; 4. *Guttulapollenites hannonicus* Goubin, 1965, Borehole CIMT-014, Sample MQ 156, Slide 1b-34, MC 1320-245, EF A33/3; 5. *Platysaccus queenslandi* de Jersey, 1962, Borehole CIMT-014, Sample MQ 111, Slide 2b-58, MC1295-185, EF H30/2; 6. *Guttulapollenites hannonicus* Goubin, 1965, Sondagem Borehole A1TM-039, Sample MQ 232, Slide 2b-4, MC1315-125, EF O32; 7. *Densipollenites? sp.*, Borehole CIMT-014, Sample MQ 111, Slide 3a-31, MC1425-55, EF V43/4; 8. *Gnetaceapollenites sinuosus* (Balme and Hennelly) Bharadwaj and Srivastava, 1969, Borehole CIMT-014, Sample MQ 147, Slide 1a-140, MC1373-41, EF W38/3.

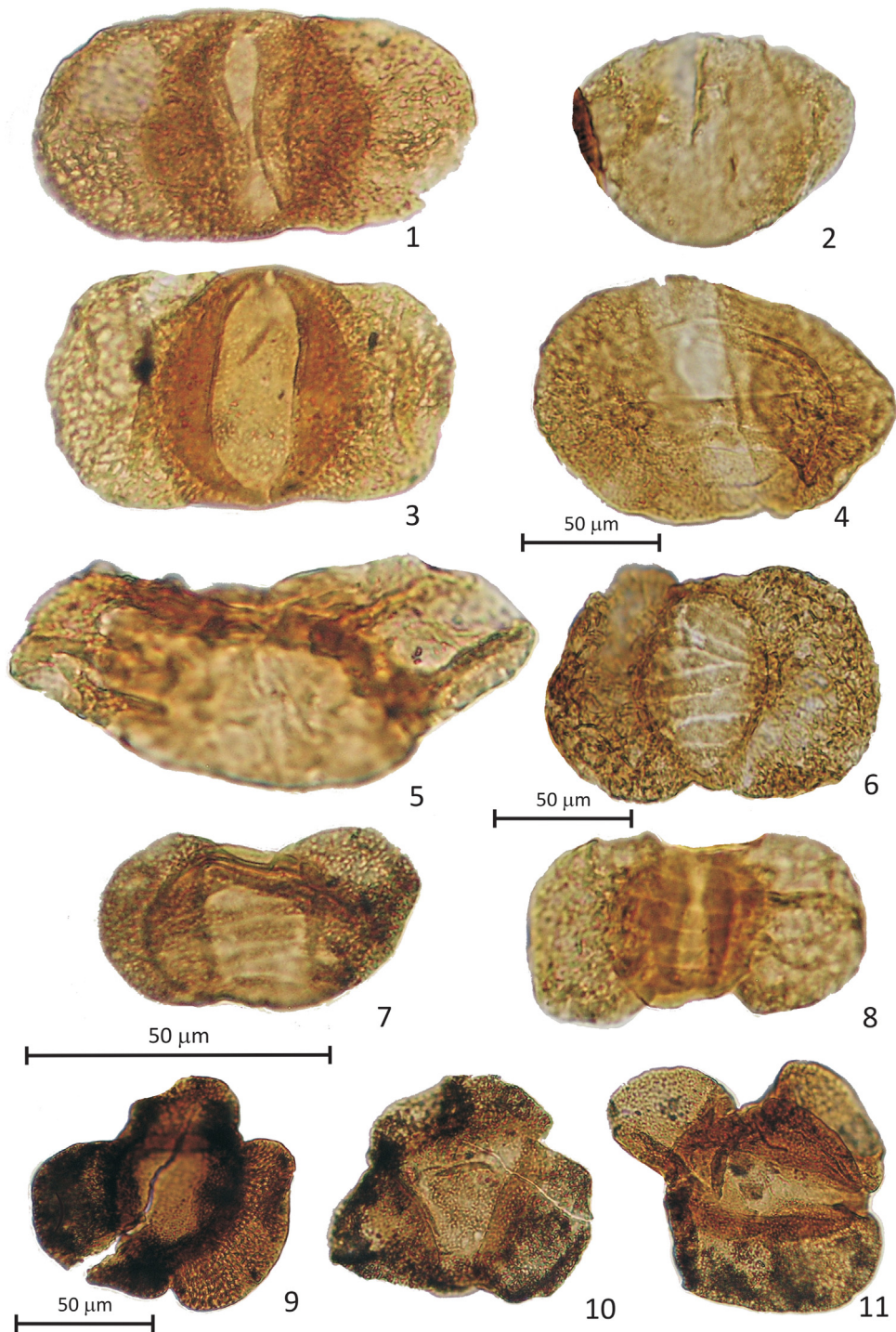


**Plate 5.** Selected palynomorph specimens from the N'Condédzi sub-basin, MNCB, Mozambique. Plate captions give the taxonomic name of the figured specimen, followed by borehole reference, sample number, slide number and microscope coordinates (MC). Scale bars: 50 µm. 1. *Falcisporites stabilis* Balme, 1970, Borehole CIMT-014, Sample MQ 111, Slide 2a-108, MC1375-95, EF R38; 2. *Klausipollenites schaubergeri* (Potonié and Klaus) Jansonius, 1962, Borehole CIMT-014, Sample MQ 147, Slide 1a-108, MC1410-70, EF U42; 3. *Falcisporites stabilis* Balme, 1970, Borehole CIMT-014, Sample MQ 111, Slide 3-121, MC1055-110, EF P6/4; 4. *Lunatisporites pellucidus* (Goubin) Helby, 1972, Borehole CIMT-014, Sample MQ 156, Slide 2a (56), MC1315-50, EF W32/2; 5. *Samaropollenites speciosus* Goubin, 1965, Borehole A1TM-039, Sample MQ 232, Slide 2-136, MC1310-110, EF P32/3; 6. *Protohaploxypinus microcorpis* (Schaarschmidt) Clarke, 1965, Borehole CIMT-014, Sample MQ 156, Slide 2a (62), MC1205-40, EF X21; 7. *Striatoabieites multistriatus* (Balme and Hennelly, 1955) Hart, 1964, Borehole CIMT-014, Sample MQ 111, Slide 3a-103, MC1130-125, EF O13/1; 8. *Striatopodocarpidites cancellatus* (Balme and Hennelly) Hart, 1964, Borehole CIMT-014, Sample MQ 148, Slide 1b-53, MC 1350-100, EF R36/2; 9. *Triadispora* sp., Borehole CIMT-014, Sample MQ 111, Slide 2b-61, MC 1300-195, EF 31/1; 10. *Triadispora crassa* Klaus, 1964, Borehole CIMT-014, Sample MQ 111, Slide 1a-165, MC 1305-138, EF O31; 11. *Triadispora crassa* Klaus, 1964, Borehole CIMT-014, Sample MQ 111, Slide 4-93, MC 1170-200, EF F17/3.

spp., *Cyclogranisporites* sp., *Horriditriletes* spp., *Laevigatosporites* spp., *Leiotriletes* sp., *Microbaculispora trisina*, *Microbaculispora* sp., *Microgranulatisporites* sp., *Punctatisporites* sp., *Retusotriletes* sp. and *Verrucosisporites andersonii* become more frequent within this interval. Common to abundant monoete spores include *Polypodiisporites* sp. and *Thymospora pseudothiessenii*, the latter occurring for the first time in this assemblage (Tables 2 and 3).

Occurrence: Borehole A1TM-058, sample interval MQ85 to MQ69 (barren sample below MQ68).

### 5.3. Assemblage L3

This assemblage is characterised by a dominance of spores, in general presenting a better preservation than the pollen grains. The most common taxa include *Apiculatisporis* sp., *Baculatisporites bharadwaji*, *Baculatisporites* sp., *Calamospora* sp., *Cyclogranisporites* sp., *Horriditriletes* spp. (common *H. tereteangulatus* and rare *H. ramosus*), *Leiotriletes* sp., *Microbaculispora* sp., *Microgranulatisporites* sp. and *Verrucosisporites andersonii* and the monoete taxa *Laevigatosporites* spp. (*L. colliensis*, and *L. vulgaris*), *Thymospora pseudothiessenii* and *Polypodiisporites* sp. Common *Lophotriletes* sp., *Osmundacidites senectus*, *Osmundacidites* sp. and *Kraeuselisporites* sp. occur here for the first time.

The assemblage is complemented with common to abundant non-taeniate and taeniate bisaccate pollen grains such as *Protohaploxylinus* spp., *Striatopodocarpites* spp. (starting to decline within this assemblage) and *Alisporites* spp., together with rare to common *Guttulapollenites hannonicus*, *Corisaccites* sp. and *Lueckisporites virkkiae*. More scarcely, *Limitisporites* sp. and *Platysaccus* sp. are also present in the assemblage. The more common colpate pollen taxa are *Gnetaceaepollenites sinuosus*, *Tiwarisporites* sp., *Vittatina* spp., *Weylandites lucifer* and *Weylandites magmus*. Rare monosaccate pollen grains are also present (e.g., *Cannanoropolis* sp.).

*Osmundacidites senectus* and rare *Protohaploxylinus microcorpus* commonly occur together throughout assemblage L3 for the first time (Table 1). The upper part of assemblage L3 is marked by the first appearance of *Klausipollenites schaubergeri*.

Occurrence: Borehole A1TM-058, sample interval MQ68 to MQ45; Borehole CIMT-014, sample interval MQ 156 to MQ 148.

### 5.4. Assemblage T1

This assemblage is characterised by an increased abundance of the following spore taxa: *Cyclogranisporites areosus*, *Granulatisporites* sp., *Horriditriletes tereteangulatus*, *Leiotriletes* sp., *Lophotriletes novicus*, *Osmundacidites senectus*, *Thymospora pseudothiessenii* and *Verrucatisporites* sp. For the first time, the occurrence of rare to common *Aratrisporites* sp., *Densoisporites neburgii*, *D. playfordii*, *Densoisporites* sp., *Lundbladispota* sp., *Playfordiaspora cancellosa* and *Verrucosisporites narmianus* is also a characteristic feature in this assemblage. The assemblage is complemented with common non-taeniate and taeniate bisaccate pollen grains such as *Alisporites* spp. and very rare *Protohaploxylinus* spp. (including rare *Protohaploxylinus microcorpus*). *Cycadopytes* sp., *Corisaccites* sp., *Gnetaceaepollenites sinuosus*, *Guttulapollenites hannonicus*, *Hamiapollenites* sp., *Lueckisporites virkkiae*, *Lunatisporites pellucidus*, *L. noviaulensis*, *Lunatisporites* sp., *Klausipollenites schaubergeri* and *Weylandites lucifer* also occur in the assemblage. Specimens of the genera *Striatopodocarpites* spp. and *Protohaploxylinus* spp. disappear within this assemblage and is associated to the last occurrence of the coal beds just below assemblage T1.

Occurrence: Borehole CIMT-014, sample MQ147 to MQ141.

### 5.5. Assemblage T2

The assemblage is characterised by the increase in abundance of the following pollen taxa *Alisporites* spp. (*A. landianus*, *A. parvus* and *A. tenuicarpus*) and *Falcisporites* spp. (*F. stabilis* and *Falcisporites* sp.), complemented by the occurrence of *Cycadopytes* sp., *Densipollenites* sp., *Hamiapollenites* sp. and *Platysaccus queenslandi*. Rare *Gnetaceaepollenites sinuosus*, *Protohaploxylinus microcorpus*, *Lueckisporites virkkiae* and *Corisaccites* sp. also extend their range into this assemblage. Rare to common *Lunatisporites pellucidus*, *L. noviaulensis*, *Klausipollenites schaubergeri* and *Hamiapollenites* spp. are also present in the assemblage (Table 3).

Common species from the preceding assemblages, as for instance, *Protohaploxylinus limpidus*, *Striatopodocarpites cancellatus*, *Guttulapollenites hannonicus* and *Weylandites lucifer*, have their last occurrence in this assemblage.

The spores are common to abundant, particularly *Aratrisporites* sp., *Calamospora landiana*, *Cyclogranisporites* sp., *Densoisporites complicatus*, *D. neburgii*, *D. playfordii*, *Densoisporites* sp., *Leiotriletes adnatus*, *Lophotriletes novicus*, *Lundbladispota* spp., *Osmundacidites senectus*, *Playfordiaspora cancellosa*, *Punctatisporites* spp. and *Verrucosisporites narmianus*.

The presence of common to rare *Convolutispora* sp., *Leiotriletes directus* and *Microbaculatisporites* sp., as well as common to abundant *Polypodiisporites* sp. and *Thymospora* sp. are interpreted as reworked. Spore UV fluorescence analysis on non-oxidized palynological residues confirms this feature. The reworked spores show dark orange fluorescence colours or have no fluorescence, whereas the indigenous palynomorph population shows intense yellow fluorescence colour, indicating lower organic maturation levels than the reworked population (Galasso et al., 2019).

Occurrence: Borehole CIMT-014, sample MQ 127 to MQ 115.

### 5.6. Assemblage T3

This assemblage is characterised by the common presence of pollen grains such as *Alisporites* spp. (*A. landianus*, *A. parvus* and *A. tenuicarpus*), *Falcisporites* spp. (*F. stabilis* and *Falcisporites* sp.) and very rare *Protohaploxylinus microcorpus*. Rare *Densipollenites* spp., *Hamiapollenites insolitus* and *Samarapollenites speciosus*, as well as common *Hamiapollenites* sp., *Platysaccus queenslandi*, *Vittatina* spp. and *Weylandites magmus* are also present in this assemblage.

Rare monosaccate pollen grains were also observed (*Striatomonosaccites ovatus Cannanoropolis* sp., *Triadispora crassa* and *Triadispora* sp.). The samples of borehole A1TM-039 also contain rare *Enzonalsporites vigens* (Table 3).

The spores assemblage is marked by the income of new species such as *Anapiculatisporites spiniger* (= *Carnisporites anteriscus*), *Anapiculatisporites* sp., *Cingutriletes* sp., cf. *Dictyophyllidites* sp., *Leiotriletes adnatus*, *Leptolepidites* sp., *Limatulasporites limatulus*, *Lundbladispota obsoleta*, *Nevesisporites fossulatus*, *Stereisporites* sp., *Striatella seebergensis*, *Striatella* sp. and *Taurocusporites* sp. Rare *Aratrisporites* sp., *Calamospora landiana*, *Cyclogranisporites* sp., *Lophotriletes novicus*, *Densoisporites* spp., *Lundbladispota brevicula*, *Playfordiaspora cancellosa*, *Verrucosisporites narmianus* and *Verrucatisporites* sp. are observed in the assemblage.

*Cyclogranisporites* sp., *Leiotriletes* sp., *Pyramidosporites* sp., *Microbaculispora* sp. and *Verrucosisporites* sp., *Verrucosisporites andersonii* are rare, and *Osmundacidites senectus*, *Polypodiisporites* sp. and *Thymospora* spp., commonly present, are all interpreted as reworked. Similar to what was observed in the previous assemblage (T2), in non-oxidized palynological residues, the reworked palynomorph population shows dark orange fluorescence colours or no fluorescence. Again, this feature is in clear contrast with the bright yellow fluorescence colours of the indigenous palynomorph population (Galasso et al., 2019).

Occurrence: Borehole CIMT-014, sample MQ 111; Borehole A1TM-039, sample interval MQ233 to MQ 231.

All assemblages present rare specimens of algae and *incertae sedis*, including *Peltacystia venosa* and *Peltacystia* sp. (Zygnemataceae algae), as well as *Cymatiosphaera gondwanensis*, *Mehlisphaeridium* sp. and *Leiosphaeridia* sp. (Prasinophyceae algae; Riboulleau et al., 2018; Spina et al., 2018a), and rare *Reduviasporonites chalastus* (*incertae sedis* organic microfossil, Spina et al., 2015, 2018b). Several fungal remains (hyphae) and root hairs are also observed.

## 6. Palynostratigraphic age interpretations

The N'Condézi sub-basin palynomorph assemblages identified in the present research are assigned to the Lopingian (late Permian), Lower Triassic, and reach the basal Upper Triassic (Carnian). The present study not only confirms the three assemblages proposed by Pereira et al. (2019) for the Lopingian sediments of the Muarâdzi sub-basin but also allowed the characterization of three new assemblages of Triassic age. Assemblage L1 is characterised by the prominence of taeniate bisaccate *Protohaploxylinus* spp. and *Striatopodocarpites* spp., as well as the non-taeniate *Alisporites* spp., which are long ranging taxa. The abundant occurrence of *Guttulapollenites* and *Weylandites* is a defining feature in this assemblage. To this assemblage, a possible early Lopingian age is assigned (Fig. 4).

Assemblage L2 is marked by the FO of *Thymospora pseudothymosporae* and includes as other characteristic taxa *Indotriradites* sp., *Kraeuselisporites* spp. and *Polypodisporites* spp. (Fig. 4). These taxa occur for the first time in this assemblage. A mid Lopingian age could be assigned to this assemblage.

Assemblage L3 is defined by the FO of *Osmundacidites senectus*, *Klausipollenites schaubergeri* and rare *Protohaploxylinus microcorpus* (Fig. 4), completes the assemblage the taxa described for the two preceding assemblages. This assemblage could be assigned to late Lopingian.

Assemblage T1 is defined by the FO of *Densoisporites neburgii* (Fig. 4). The assemblage includes *Aratrisporites* sp., *D. playfordii*, *Densoisporites* sp., *Lundbladispota* spp., *Playfordiaspora cancellosa* and *Verrucosiporites narmianus*, the latter has its FO in the assemblage. To this assemblage is assigned an Induan age (early Triassic).

Assemblage T2 presents a change in the palynomorph group abundances. The non-taeniate bisaccate gymnosperm pollens such as *Alisporites parvus*, *Falcisporites stabilis* and *Falcisporites* sp. are abundant and occur for the first time in the present assemblage (Fig. 4). The FO of *Platysaccus queenslandi* and *Densipollenites* sp. is also observed (Fig. 4). This assemblage could be assigned to Olenekian (Lower Triassic). The assemblage is also characterised by the disappearance of important species such as *Alisporites plicatus*, *Cannanoropollis* sp., *Guttulapollenites hannonicus*, *Protohaploxylinus limpidus*, *Striatopodocarpites cancellatus*, *Vittatina* sp. and *Weylandites lucifer*.

In assemblage T3, *Anapiculatisporites spiniger* (= *Carnisporites anteriscus*), cf. *Dictyophyllidites* sp., *Leiotriletes adnatus*, *Leptolepidites* sp., *Limatulasporites limatulus*, *Lundbladispota obsoleta*, *Nevesisporites fossulatus*, *Stereisporites* sp., *Striatella seebergensis*, *Striatella* sp. and *Taurocusporites* sp., as well as rare *Samaropollenites speciosus* and *Enzonalasporites vigens* occur for the first time (Fig. 4). This assemblage is assigned to Carnian.

Assemblages T2 and T3 present common reworked spores of Lopingian age or older (*Cyclogranisporites* sp., *Osmundacidites senectus*, *Polypodisporites* sp. and *Thymospora* sp.). This feature was confirmed by the UV fluorescence colour of the non-oxidized spores, and permitted to identify and confirm an erosive episode that occurred in the MMEB during the Middle Triassic (Fernandes

et al., 2015; Galasso et al., 2019). The identification of palynomorphs reworking is critical (Lindström and McLoughlin, 2007; di Pasquo et al., 2017) in particular in the stratigraphic sequences related to mass-extinctions events, as for instance the Permian-Triassic Boundary (PTB). *Osmundacidites senectus* appears not to have been greatly affected by the PTB extinction-event as it is corroborated by different studies in other localities, e.g., Antarctica (Lindström and McLoughlin, 2007) and Madagascar (Msaky and Srivastava, 1997), it is common in the late Permian of Gondwana, presenting a great decline in the early Triassic. Other species such as *Lophotriletes* sp. and *Leiotriletes directus* are also present throughout PTB time interval (Lindström and McLoughlin, 2007) but not present in Upper Triassic. In the MMEB, the common presence of these taxa in the Upper Triassic sedimentary rocks is interpreted as reworked inferred from UV spore fluorescence colours (Galasso et al., 2019), being an independent tool to estimate the degree of reworking at these ages.

## 7. Stratigraphical significance of the palynoflora and correlations across Gondwana

The palynostratigraphic characterisation of the PTB across the Gondwana Supercontinent has been a matter of debate for a long time. The typical microflora of dominant gymnosperms pollen vegetation, at the end of the Permian period, change to the abundant lycopphyte spore producing vegetation, in the early Triassic, has been discussed by several authors (Steiner et al., 2003; Lindström and McLoughlin, 2007; Pereira et al., 2016). The latest Permian palynostratigraphic correlation synthesis across Gondwana is presented in Pereira et al. (2019). Thus, the present paper will discuss the correlations of the PT boundary (also described in Pereira et al., 2016), as well as of the Lower and Upper Triassic. The palynofloral record from MMEB shows a discrete floral change at the PT boundary. The spore and pollen diversity presents some decrease during the lowermost Triassic and the assemblages show a mixed Permian-Triassic feature, composed of common gymnosperms pollen and lycopphyte spore with the income of new spore taxa. This fact is observed in other central Gondwana PT boundary sections as for instance Kenya, Tanzania, Zambia, South Africa, Madagascar, Pakistan, and Antarctica (Lindström and McLoughlin, 2007; Hochuli et al., 2010; Hermann et al., 2012; Hermann and Bucher, 2015) and also in other palaeogeographic areas (e.g., Italy, Southern Alps, Cirilli et al., 1998; Spina et al., 2015).

Although independent age constrains are missing in this study, the assemblages described are tentatively correlated with the stratigraphic records of different Karoo basins already studied in Mozambique (Pereira et al., 2016, 2019). The Lopingian main assemblages (L1, L2 and L3) recognized in the N'Condézi sub-basin perfectly correlate with the assemblages established for the Muarâdzi sub-basin (Pereira et al., 2019). This characteristic indicates that the palynostratigraphy of the sub-basins can be easily correlated across the MMEB.

According to Foster et al. (1998) and Lindström and McLoughlin (2007), the late Lopingian key-taxa of the PT boundary in Gondwana are *Lunatisporites pellucidus* and *Aratrisporites* spp. However, *Aratrisporites* spp. can be considered facies dependent (Retallack, 1977).

In Mozambique, *L. pellucidus* occurs infrequently in the latest Permian, becoming more abundant in the early Triassic assemblages. The early Induan is marked by the FO of *Densoisporites neburgii* and *Aratrisporites* sp. Neither of these key-taxa is very abundant in the studied sections, but both occur for the first time in the lowermost Triassic successions (Borehole CIMT-014 and Fig. 4). The following Olenekian interpreted age assemblage (Assemblage T2) is marked by the income of new pollen

species (*Alisporites parvus*, *Falcisporites stabilis*, *Falcisporites* spp. and *Platysaccus queenslandi*) (Fig. 4), as well as common spores such as *Densoisporites complicatus*, *Leiotriletes adnatus* and *Lundbladispora obsoleta*.

In the Lower Triassic of central Gondwana, other significant species defining the lowermost boundary are *Playfordiaspora cancellosa* and *Triplexisporites playfordii* (Wright and Askin, 1987; Hankel, 1993; Foster et al., 1994; Lindström and McLoughlin, 2007). *Playfordiaspora cancellosa* is rare to common in the early Triassic in Mozambique, and *Triplexisporites playfordii* was never recovered in this study, as well as in other MNCB palynological studies (Pereira et al., 2016).

### 7.1. The late Permian and the early Triassic

The latest Permian-Triassic palynomorph assemblages in Central Gondwana, studied in Kenya (Hankel, 1992), presents an assemblage dominated by taeniata bisaccate pollen. The lowermost Triassic succession is missing, but the early Triassic characteristic taxa present are *Densoisporites* sp., *Lunatisporites pellucidus*, *Lundbladispora willmottii*, *Playfordiaspora cancellosa*, *Protohaploxylinus microcorpus* and *Triplexisporites playfordii*. In Kenya, *T. playfordii* and *P. cancellosa* are not recorded in the early Triassic assemblages, but they occur in a younger assemblage (Hankel, 1991, 1992). The Induan assemblage in Kenya is very similar to the Assemblage T1 described in this study for the N'Condédzi sub-basin succession.

In Tanzania (Hankel, 1987; Msaky and Srivastava, 1997), the PT boundary is present in the Hatambulo Formation and is marked by the occurrences of common *Lueckisporites* sp., *Guttulapollenites hannonicus*, *Striatopodocarpites* spp. and *Protohaploxylinus* spp. (late Permian), as well as *Alisporites* sp., *Apiculatisporites* sp., *Densipollenites* sp., *Playfordiaspora cancellosa* and *Platysaccus* sp. This association is also very similar to the Assemblage T1 described for the N'Condédzi sub-basin succession, whereas *Playfordiaspora cancellosa* is recorded in the late Middle Triassic of Tanzania.

In southern Zambia (Mid-Zambezi Valley section), the late Permian assemblages include *Guttulapollenites hannonicus*, *Thymospora pseudothiessenii* and *Weylandites lucifer*, that can be correlated with Assemblage L2 of late Wuchiapingian age, in the Muarádzi and the N'Condédzi sub-basins (Pereira et al., submit; and in this study). The early Triassic is missing in this region, but then the late Lower Triassic (Olenekian) is marked by the presence of *Alisporites* spp., *Aratrisporites ficheri*, *Falcisporites stabilis*, *Lunatisporites pellucidus*, *Platysaccus queenslandii*, *Playfordiaspora cancellosa*, *Sulcatisporites* sp., *Uvaesporites* sp. and *Verrucosisporites* sp. (Nyambe and Utting, 1997). The assemblage closely resembles the Assemblage T2 described in this study for the N'Condédzi sub-basin.

To the latest Permian sequence in Zimbabwe (Mid-Zambezi Basin) Zone IV, Subzones H and H1 (*Protohaploxylinus* sub-assemblage) are assigned. The early Triassic succession is characterised by the transitional *Protohaploxylinus-Alisporites* spp. assemblage (Falcon, 1975; Falcon et al., 1984). The correlation with the Muarádzi and the N'Condédzi sub-basins remains difficult.

In South Africa, according to Steiner et al. (2003), the late Permian-early Triassic zonation includes two biozones: the *Klausipollenites schaubergeri* Zone, which is characterised by *Falcisporites* spp., *Playfordiaspora cancellosa*, *Protohaploxylinus* sp. and *Triplexisporites playfordii* (these two last species are common in the late Permian, but are not recorded in the early Triassic in this region), and the *Kraeuselisporites-Lunatisporites* Zone, dominated by lycopsid species such as *Kraeuselisporites* spp., *Lundbladispora* spp. and *Lunatisporites* spp. (including *L. pellucidus* and *L. noviaulensis*). The *Klausipollenites schaubergeri* zone is clearly different from

the assemblages described from Mozambique (suggested in this study and in Pereira et al., 2019). Even so, the *Kraeuselisporites-Lunatisporites* zone enables a comprehensive correlation with the early Triassic Assemblage T1, based on the presence of *Lundbladispora* spp., and *Lunatisporites* spp.; however, key species recorded in the N'Condédzi sub-basin are missing in South Africa, such as *Densoisporites neburgii* and *Aratrisporites* spp.

The upper Triassic successions of Madagascar (Gobin, 1965; Wright and Askin, 1987; Hankel, 1993) comprise common to abundant *Lunatisporites pellucidus* (occurring for the first time in latest Permian) and an increase in the abundance of *Striatopodocarpites pantii*. Common *Protohaploxylinus* spp. and lycopsid spores such as *Densoisporites* spp., *Lundbladispora* sp., *Kraeuselisporites* spp. (mostly in the lower part), as well as *Ephedripites* sp., *Limatulasporites fossulatus*, *Playfordiaspora cancellosa*, *Striomonosaccites morondavensis*, and *Triplexisporites playfordii* and rare *Guttulapollenites hannonicus* and *Weylandites* spp. are also part of the assemblage. This assemblage can be correlated with the Assemblage T1 described in the N'Condédzi sub-basin, except for the presence of *Triplexisporites playfordii*, which was never recorded in the MNCB successions.

In Pakistan (Balme, 1970; Hermann et al., 2012; Hermann and Bucher, 2015), the Permian-Triassic succession at Amb, Salt Range, is characterised by the occurrence of *Acanthotriletes tereteangulatus*, *Dictyophyllidites harrisii*, *Falcisporites australis*, *Kraeuselisporites* spp., *Guttulapollenites hannonicus*, *Protohaploxylinus* spp. (including *P. microcorpus*), *Triquitrites proratus* and *Sulcatisporites ovatus*. The early Triassic assemblage contains several typical Permian taxa, as well as new Triassic taxa such as *Protohaploxylinus varius*, *Cycadopites* spp., *Densoisporites* spp. and *Lunatisporites* spp., *Lundbladispora* spp., that could be direct correlated with the Assemblage T1 described in the N'Condédzi sub-basin. *Triplexisporites playfordii* was not recorded in the early Triassic assemblages of Pakistan but occurs higher in the stratigraphic section (Balme, 1970; Hermann et al., 2012; Hermann and Bucher, 2015). *Playfordiaspora cancellosa* is observed also in the early Triassic (Balme, 1970) and is comparable to the N'Condédzi sub-basins record.

In India, several studies (e.g., Srivastava and Jha, 1990; Jha and Srivastava, 1996; Jha, 2006; Jha et al., 2018) describe in the early Triassic the palynoassemblage X, which is characterised by the increase in the *Lunatisporites* species, and the decline in the percentage of striate bisaccate pollen grains (such as *Striatopodocarpites* spp. and *Faunipollenites* spp.). The assemblage also contains *Crescentipollenites*, *Densipollenites*, *Klausipollenites*, *Alisporites* and *Lundbladispora*. Palynoassemblage XI (Olenekian age) is characterised by the dominance of *Lundbladispora* spp. and *Densoisporites* spp., along with the occurrence of *Striatopodocarpites* spp., *Faunipollenites* spp. and *Crescentipollenites* spp. The stratigraphically significant taxa of this palynoassemblage are *Araucariacites* sp., *Brachysaccus ovalis*, *Chordasporites* sp., *Falcisporites nuthallensis*, *Klausipollenites schaubergeri*, *Playfordiaspora cancellosa*, *Ringosporites fossulatus* and *Staurosaccites marginalis*. Tentatively, the assemblage correlation with Assemblage T1 is based on common presence of *Lundbladispora* spp. and *Densoisporites* spp.

In the Prince Charles Mountain succession, in Antarctica (Foster et al., 1994; Lindström and McLoughlin, 2007), the early Triassic succession is marked by the occurrence of *Lunatisporites* spp., *Protohaploxylinus microcorpus*, *P. samoilovichii*, *Falcisporites* spp. and *Alisporites* spp., with common *Brevitriletes* spp., *Leiotriletes directus*, *Osmundacidites* spp. and *Dictyophyllidites* spp. A high diversity and abundance of lycopsid spores, mainly *Densoisporites* spp. (*Densoisporites neburgii*), *Lundbladispora* spp., *Kraeuselisporites* spp. and *Uvaesporites* spp. was also registered. This latter assemblage can be correlated with Assemblage T1 described for the N'Condédzi sub-basin. *T. playfordii* and *P. cancellosa* are not observed in these late

Permian successions; however, their first appearance occur in early Triassic rocks.

### 7.2. The Upper Triassic

The Carnian palynoflora of Gondwana is constrained by latitudinal and climatic factors, showing a distinct provincialism (Artabe et al., 2003; Dolby and Balme, 1976; Foster et al., 1994; Buratti and Cirilli, 2007; Cirilli, 2010), with two major palynofloral provinces recognized in the southern hemisphere: the Onslow and the Ipswich microflora.

The Onslow microflora is recognized in Northwestern Australia, Timor, extending through the western Tethys coasts (e.g., present coordinates north and eastern Africa, Sicily, Tunisia, Libya, Israel, India and Madagascar) and Western Europe, representing a warm temperate climate that established along these continental margins (Foster et al., 1994; Dolby and Balme, 1976; Buratti and Cirilli, 2007; Cirilli, 2010; Césari and Colombi, 2013, 2016; Cirilli et al., 2015, 2018). This microflora is characterised by the presence of mixed taxa typical of Northern Europe and South Gondwana, comprising the following taxa: *Aulisporites*, *Camerospirites*, *Enzonasporites*, *Duplexisporites*, *Infernopollenites*, *Minutosaccus*, *Ovalipollis*, *Samaropollenites* and *Weylandites*, species typical of warm temperate climates. All of these species are absent in the Ipswich Microflora, which is characterised by the presence of taxa typical of cool temperate climate. Ipswich Microflora is depicted by the abundance of bisaccate pollen, monosulcate pollen and trilete spores. The Ipswich Microflora extends from southern and eastern Australia, Antarctica, South Africa and the Western margin of South America (Argentina and Chile).

The key species for the Carnian Onslow Microflora are *Samarisporites speciosus* and *Enzonasporites vigens* (Dolby and Balme, 1976; Cirilli, 2010). In East India (Tripathi and Raychowdhuri, 2005), it has been correlated with the *Rimaesporites pottoniei/Samaropollenites speciosus* Assemblage Zone of the Godavari Basin (Prasad, 1997). Hankel (1987) recognized the *Staurosaccites quadrifidus* Microflora, *Samaropollenites speciosus* and *Minutosaccus crenulatus* Microflora of Carnian-early Norian age in Tanzania (Luwegu Basin). These palynofloras could be correlated with *Samaropollenites speciosus* defined by Dolby and Balme (1976) in Western Australia.

In Mozambique, a Carnian assemblage was identified for the first time in two boreholes (boreholes CIMT-014 and A1TM-039) (Fig. 3) and presents several similarities with the Onslow Microflora. The significant species present are *Samarisporites speciosus* and *Enzonasporites vigens*, assorted with distinctive cosmopolitan species (*Anapiculatisporites spiniger/Carnisporites anteriscus*, cf. *Dictyophylidites* sp., *Limatulasporites limatulus*, *Nevesisporites fossulatus*, *Stereisporites* sp., *Striatella seebergensis*, *Striatella* sp. and *Taurocuporites* sp.). All these taxa are recorded for the first time in the upper Triassic successions in Mozambique, allowing the recognition of a mixed signature microflora. These results are preliminary, and ongoing studies have to confirm and better characterise this feature.

## 8. Stratigraphic record and its implication to interbasinal correlation

Conglomerates positioned immediately above the basement rocks in the Mozambican Karoo basins are frequently attributed to the Vúzi Formation (GTK Consortium, 2006) and are interpreted as tillites or fluvio-glacial deposits resulting from the end Carboniferous-early Permian Gondwana glaciation. The Vúzi Formation is correlated to the top of the Dwyka Group of the Main Karoo Basin, and therefore, a late Carboniferous to early Permian

age is attributed to this formation based only on lateral lithological correlations (GTK Consortium, 2006; Paulino et al., 2010; Lakshminarayana, 2015). However, the presence of red clastic lithologies between the basement rocks and the conglomerates (A1TM-058), suggests deposition under more temperate climatic conditions in an oxidizing sub-aerial environment rather than glacial to periglacial environments. Moreover, the conglomerate beds identified in the Muarádzi sub-basin ranging in age from the Cisuralian-Guadalupian boundary (Lopes et al., 2014; Pereira et al., 2014) to Lopingian in borehole A1TM-058 and others boreholes (Pereira et al., 2019) indicate that there are several conglomerate beds of different ages intercalated in the stratigraphic successions of the Moatize and Matinde formations. Therefore, not all conglomerate beds positioned immediately above the basement are the product of glacial processes. If all conglomerate beds found in the last stratigraphic position are considered glacial deposits, glacial environments persisted in this region until the Lopingian, which is unlikely and not documented in any of the other Gondwana basins of Southeast Africa (Wopfner, 1999; Catuneanu et al., 2005). The palynological age of the conglomerate beds located immediately above crystalline basement rocks (Lopes et al., 2014; Pereira et al., 2014, 2016, 2019) indicates that not all of these sedimentary rocks should be considered as part of the Vúzi Formation. Therefore, we consider that the conglomerates at the base of borehole A1TM-058 could correspond to syntectonic sediments of Lopingian age, which probably marks the main phase of faulting within tectono-structural development of the basin. Accordingly, these conglomerates could represent coarse clastic sedimentary rocks deposited in alluvial fans that formed at the toe of the normal faults delimiting this Karoo Mozambique basin. This assumption also implies that conglomerate beds cannot be used as marker beds used for separating the different lithostratigraphic formations as they occurs interbedded both in the successions of the Moatize and Matinde formations. Thus, a better, clearer and formal definition for the stratigraphic boundary between these two units is needed. For example, if the conglomerate beds present at the base of borehole A1TM-058 (Fig. 3) were considered the base of the Matinde Formation, the minimum thickness for the latter formation is, therefore, ca. 1000 m, which is the measured succession of the borehole and coal deposition persisted in this sub-basin until the end-Permian. However, if the conglomerate beds of the same borehole were considered the Vúzi Formation, the ca. 1000 m of coal-bearing sedimentary rocks above belong to the Moatize Formation. Because there are no major lithological changes in this ca. 1000 m thick succession, it is impossible to identify and place the boundary between the Moatize and Matinde formations within this succession.

The change from coal depositional environments to red beds successions, observed at the bottom of borehole CIMT-014 (Fig. 3), marks an important change in the depositional environments and palaeoclimatic conditions, which coincides approximately, with the Permo-Triassic boundary. According to the palynological studies done in the MMCB (Lopes et al., 2014; Pereira et al., 2014, 2016, 2019), this PT boundary also establishes the limit between the Matinde and the Cádzi formations. Therefore, most of the succession of borehole CIMT-014, as well as all the succession of borehole A1TM-039, belong to the Cádzi Formation. Within the Cádzi Formation, after the red bed deposition in the early Triassic, a phase of erosion occurred, marked by a Middle Triassic hiatus, followed by the deposition of upper Triassic red beds dated by palynomorphs, together with reworked Permian palynomorphs, probably sourced from the nearest Karoo basins (Galasso et al., 2019). The Cádzi Formation red beds succession of Triassic age yielded some rich spore levels, which could be associated to the increase of seasonal rainfall episodes or to possible changes in the river systems (from meandering to braided) (Ward et al., 2000).

Tectonics and palaeoclimates were the main factors responsible for the different lithofacies recorded in the Permo-Triassic Karoo basins (Catuneanu et al., 2005). The high sedimentation rates observed in the Mozambique Karoo basins lead to the accumulation of more than 2000 m thick sediments, in coal-bearing swamps environments associated with fluvio-deltaic depositional systems in Late Permian times. The change to hot and arid climate conditions with fluctuating precipitation, related to red bed environments, occurred during the early Triassic in Mozambique. The Middle Triassic hiatus event, identified in Mozambique (Fernandes et al., 2015), can be correlated across the Karoo rift basins of East Africa (Tanzania, Kenya, Zambia, Mozambique, Madagascar), representing an important tectonic event in the development of these Karoo basins. This tectonic event observed in the East African/Madagascar region is characterized by a general uplift and erosion of the Karoo basins, and was followed by another major rifting event in the Late Triassic. This unique tectonic event set it apart from all other Karoo-age basins of Africa, in particular from the Main Karoo Basin of South Africa, which depositional history is related to the development of a foreland basin formed by the tectonic load of the Cape Fold Belt. The differences in the tectonic style between the Main Karoo Basin and the East Africa rift basins should be emphasized and could have affected the FOs of the key-taxa hampering the establishment of robust correlation schemes across central Gondwana.

## 9. Conclusions

The main results from this study are summarized below:

- in N'Condédzi sub-basin of MNCB, the Matinde Formation succession is dated late Permian (Lopingian) and the Cádzi Formation is dated Lower Triassic to Upper Triassic. No Middle Triassic rocks were recognized; therefore, the contact between the Lower and the Upper Triassic sedimentary rocks could correspond to a major hiatus;
- the Lopingian age is defined in detail based on three main palyno-assemblages (Assemblage L1 based in FO of *Guttulapollenites* pollen; Assemblage L2 is marked by the FO of *Thymospora pseudothiessenii* and Assemblage L3 is defined by the FO of *Osmundacidites senectus*);
- Lopingian palyno-assemblages recovered in N'Condédzi sub-basin correlate fully with the palyno-assemblages recovered in the Muarádzi sub-basin of the MNCB;
- palynomorphs of Triassic age were identified for the first time in the Mozambican Karoo basins. This study allowed the identification of three new Triassic assemblages: Assemblage T1 is defined by the FO of *Densoisporites nejburgii* of Induan age, Assemblage T2 is marked by the FO of *Platysaccus queenslandi* and could be assigned to the Olenekian age, and Assemblage T3 is defined by the FO of *Samaropollenites speciosus* and *Enzonalsporites vicens*, indicating a Carnian age;
- the recent biostratigraphic data obtained constrains the age of the Karoo Supergroup formations of Mozambique, and it is a major contribute to a better understanding of the palaeoecological and palaeoclimatic evolution of the basin;
- the absence of Middle Triassic sedimentary rocks, identified by the study of the palynological record, correlates well with a Middle Triassic episode of uplift and erosion described by Fernandes et al. (2015) for the MNCB in the Muarádzi sub-basin. Moreover, the presence of Permian reworked palynomorphs in upper Triassic sedimentary rocks supports this Middle Triassic tectonic event;
- this study increases the knowledge of the palaeogeographic position of the Mozambique basins within the Gondwana super-continent.

## Disclosure of interest

The authors declare that they have no competing interest.

## Acknowledgments

The research was supported by the project PALEOCLIMOZ (PTDC/CTA-GEO/30082/2017). The authors would like to thank the Managers of Coal India Africana, Limitada and Gondwana Empreendimentos e Consultorias, Limitada, for borehole access and complementary information. Francesca Galasso acknowledges the University of Perugia for the opportunity to participate in the program Erasmus + Traineeship, funded by the European Commission. LNEG's technician Irene Sousa is acknowledged for laboratory support and sample preparation. Editor and the reviewers A. Gotz and M. di Pasquo are gratefully acknowledge for valuable comments that improved the manuscript.

## Appendix A. Appendix A

### List of Taxa

List of spore-pollen species identified in the studied sections of the N'Condédzi sub-basin.

- Anapiculatisporites* sp.  
*Anapiculatisporites spiniger* (Leschik) Reinhardt/*Carnisporites anteriscus* Morbey, 1975  
*Aratrisporites* sp.  
*Baculatisporites bharadwaji* Hart, 1963  
*Baculatisporites* sp.  
*Brevitriletes cornutus* (Balme and Hennelly) Backhouse, 1991  
*Brevitriletes* sp.  
*Calamospora landiana* Balme, 1970  
*Calamospora rugosa* (Ibrahim) Schopf, Wilson and Bentall, 1944  
*Calamospora* sp.  
 cf. *Dictyophyllidites* sp.  
*Convolutispora* sp.  
*Cyclogranisporites* sp.  
*Densoisporites complicatus* Balme, 1970  
*Densoisporites nejburgii* (Schulz) Balme, 1970  
*Densoisporites playfordii* (Balme) Balme, 1970  
*Densoisporites* spp.  
*Fabasporites* sp.  
*Granulatisporites* sp.  
*Horriditriletes ramosus* (Balme and Hennelly) Bharadwaj and Salujha, 1964  
*Horriditriletes tereteangulatus* (Balme and Hennelly) Backhouse, 1991  
*Horriditriletes* sp.  
*Kraeuselisporites* sp.  
*Laevigatosporites colliensis* (Bharadwaj and Hennelly) Venkatachala and Kar, 1968  
*Laevigatosporites vulgaris* (Ibrahim) Ibrahim, 1933  
*Laevigatosporites* spp.  
*Leiotriletes adnatus* (Kosanke, 1950) Potonié and Kremp, 1955  
*Leiotriletes directus* Balme and Hennelly, 1955  
*Leiotriletes* sp.  
*Leptolepidites* sp.  
*Limatulasporites limatulus* (Playford) Helby and Foster, 1979  
*Lophotriletes novicus* Singh, 1964  
*Lophotriletes* sp.  
*Lundbladispora brevicula* Balme, 1963  
*Lundbladispora* sp.  
*Microbaculatisporites* sp.  
*Microbaculispora trisina* (Balme and Hennelly) Anderson, 1977  
*Microbaculispora* sp.

*Microgranulatisporites* sp.  
*Nevesisporites fossilatus* Balme, 1970  
*Osmundacidites senectus* Balme, 1970  
*Osmundacidites* sp.  
*Playfordiaspora cancellosa* (Playford and Dettmann) Maheshwari and Banerji, 1975  
*Polypodiisporites* sp. sensu Balme, 1970  
*Polypodiisporites mutabilis* Balme, 1970  
*Procoronaspora spinosa* (Anderson) Backhouse, 1991  
*Punctatisporites* spp.  
*Pyramidosporites* sp.  
*Retusotriletes* sp.  
*Stereisporites* sp.  
*Striatella seebergensis* Madler, 1964  
*Striatella* sp.  
*Taurocusporites* sp.  
*Thymospora pseudothiessenii* (Kosanke) Wilson and Venkatachala, 1963  
*Thymospora* sp.  
*Verrucatisporites* sp.  
*Verrucosisporites andersonii* Backhouse, 1988  
*Verrucosisporites narmianus* Balme, 1970  
*Verrucosisporites* sp.

#### Pollen grains

*Alisporites landianus* Balme, 1970  
*Alisporites ovatus* (Balme and Hennelly) Jansonius, 1962  
*Alisporites parvus* de Jersey, 1962  
*Alisporites plicatus* Jizba, 1962  
*Alisporites potonie* (Lakhanpal, Sah and Dube) Somers, 1968  
*Alisporites* sp.  
*Cannanoropollis* sp.  
*Corisaccites* sp.  
*Cycadopites* sp.  
*Densipollenites* sp.  
*Enzonalsporites vigens* Leschik, 1955  
*Falcisporites stabilis* Balme, 1970  
*Gnetaceapollenites sinuosus* (Balme and Hennelly) Bharadwaj and Srivastava, 1969  
*Guttulapollenites hannonicus* Goubin, 1965  
*Hamiapollenites insolitus*  
*Hamiapollenites* sp.  
*Klausipollenites schaubergeri* (Potonié and Klaus) Jansonius, 1962  
*Limitisporites* sp.  
*Lueckisporites virkkiae* Potonié and Klaus, 1954  
*Lueckisporites* spp.  
*Lunatisporites noviaulensis* (Leschik) Foster, 1979  
*Lunatisporites pellucidus* (Goubin) Helby, 1972  
*Lunatisporites* sp.  
*Platysaccus papilionis* Potonié and Klaus, 1954  
*Platysaccus queenslandi* de Jersey, 1962  
*Platysaccus* sp.  
*Protohaploxylinus amplus* (Balme and Hennelly) Hart, 1964  
*Protohaploxylinus goraiensis* (Potonié and Lele) Hart, 1964  
*Protohaploxylinus hartii* Foster, 1979  
*Protohaploxylinus limpidus* (Balme and Hennelly) Balme and Playford, 1967  
*Protohaploxylinus microcorpus* (Schaarschmidt) Clarke, 1965  
*Protohaploxylinus* sp.  
*Samaropollenites speciosus* Goubin, 1965  
*Striatoabieites multistriatus* (Balme and Hennelly 1955) Hart, 1964  
*Striatoabieites* sp.  
*Striatomonosaccites* sp.  
*Striatopodocarpites cancellatus* (Balme and Hennelly) Hart, 1964

*Striatopodocarpites fusus* (Balme and Hennelly) Potonié, 1956  
*Striatopodocarpites gondwanensis* (Lakhanpal, Sah and Dube) Hart, 1964  
*Striatopodocarpites* sp.  
*Tiwarisporites* sp.  
*Triadispora crassa* Klaus, 1964  
*Triadispora* sp.  
*Vittatina costabilis* Wilson, 1962  
*Vittatina fasciolata* (Balme and Hennelly) Bharadwaj, 1962  
*Vittatina scutata* (Balme and Hennelly) Bharadwaj, 1962  
*Vittatina* sp.  
*Weylandites lucifer* (Bharadwaj and Salujha) Foster, 1975  
*Weylandites magmus* (Bose and Kar) Backhouse, 1991

#### Algae and incertae sedis

*Brazilea* sp. A in Backhouse, 1991  
Chlorophycean algae *incertae sedis* (sphaeromorph clusters)  
*Cymatiosphaera gondwanensis* (Tiwari) Backhouse, 1991  
*Mehlisphaeridium* sp.  
*Peltacystia venosa* Balme and Segroves, 1966  
*Reduviasporonites chalastus* (Foster) Elsik, 1999

#### Appendix B. Supplementary data

Supplementary data associated with this article can be found, in the online version, at <https://doi.org/10.1016/j.revmic.2019.05.001>.

#### References

- Afonso, R.S., 1984. Ambiente geológico dos carvões gonduânicos de Moçambique – uma síntese. In: Lemos de Sousa, M.J. (Ed.), Symposium on Gondwana Coals, Lisbon, 1983. Proceedings and Papers. Comunicações dos Serviços Geológicos de Portugal 70 (2), 205–214.
- Artabe, A.E., Morel, E.M., Spalletti, L.A., 2003. Caracterización de las provincias fitogeográficas Triásicas del Gondwana extratropical. Ameghiniana 40, 387–405.
- Balme, B.E., 1970. Palynology of Permian and Triassic strata in the Salt Range and Surghar Range, West Pakistan. In: Kummel, B., Teichert, C. (Eds.), Stratigraphic Boundary Problems: Permian and Triassic of West Pakistan. The University Press of Kansas, Lawrence, KS, pp. 305–453.
- Backhouse, J., 1991. Permian palynostratigraphy of the Collie Basin, Western Australia. Review of Palaeobotany and Palynology 67, 237–314.
- Bicca, M.M., Philipp, R.P., Jelinek, A.R., Ketzler, J.M.M., Scherer, C.M.S., Jamal, D.L., Reis, A.D., 2017. Permian-early Triassic tectonic and stratigraphy of the Karoo Supergroup in Northwestern Mozambique. Journal of African Earth Sciences 130, 8–27.
- Bicca, M.M., Jelinek, A.R., Philipp, R.P., Lana, C.C., Alkimm, A.R., 2018. Precambrian-Cambrian provenance of Matinde Formation, Karoo Supergroup, northwestern Mozambique, constrained from detrital zircon U-Pb age and Lu-Hf isotope data. Journal of African Earth Sciences 138, 42–57.
- Buratti, N., Cirilli, S., 2007. Microfloristic provincialism in the Upper Triassic Circum – Mediterranean area and palaeogeographic implication. Geobios 40, 133–142.
- Carvalho, L.H.B., 1977. Formações vulcânicas de Carinde, Tete-Moçambique. Instituto Superior Técnico, Lisboa (Unpublished Ph.D. Thesis).
- Catuneanu, O., Wopfner, H., Eriksson, P.G., Cairncross, B., Rubidge, B.S., Smith, R.M.H., Hancox, P.J., 2005. The Karoo basins of south-central Africa. Journal of African Earth Sciences 43, 211–253.
- Césari, S.N., Colombi, C.E., 2013. A new Late Triassic phytogeographical scenario in westernmost Gondwana. Nature Communications 4 (1889), 1–6.
- Césari, S.N., Colombi, C.E., 2016. Palynology of Late Triassic Ischigualasto Formation, Argentina: paleoecological and paleogeographic implications. Palaeogeography, Palaeoclimatology, Palaeoecology 449, 365–384.
- Cirilli, S., 2010. Upper Triassic lowermost Jurassic palynology and palynostratigraphy: a review. Geological Society of America Bulletin 334, 285–314.
- Cirilli, S., Pirini, C., Ponton, M., Radrizzani, S., 1998. Stratigraphical and palaeoenvironmental analysis of the Permian-Triassic transition in the Badia Valley (Southern Alps, Italy). Palaeogeography, Palaeoclimatology, Palaeoecology 138 (1–4), 85–113.
- Cirilli, S., Buratti, N., Gugliotti, L., Frixa, A., 2015. Palynostratigraphy and palynofacies of the Upper Triassic Streppenosa Formation (SE Sicily, Italy) and inference on the main controlling factors in the organic rich shale deposition. Review of palaeobotany and palynology 218, 67–79.
- Cirilli, S., Panfili, G., Buratti, N., Frixa, A., 2018. Palaeoenvironmental reconstruction by means of palynofacies and lithofacies analyses: an example from the Upper

- Triassic subsurface succession of the Hyblean Plateau Petroleum System (SE Sicily, Italy). *Review of Palaeobotany and Palynology* 253, 70–87.
- di Pasquo, M., Anderson, H., Isaacson, P., 2017. Record of a Pennsylvanian–Cisuralian marine transgression, southern Bolivia: a short-lived event in western Gondwana? *Palaeogeography, Palaeoclimatology, Palaeoecology* 485, 30–45.
- Dolby, J.H., Balme, B.E., 1976. Triassic palynology of the Carnarvon Basin, Western Australia. *Review of Palaeobotany and Palynology* 22, 105–168.
- Duncan, R.A., Hooper, P.R., Rehacek, J., Marsh, J.S., Duncan, A.R., 1997. The timing and duration of the Karoo igneous event, southern Gondwana. *Journal of Geophysical Research, Solid Earth* (1978 to 2012) 102 (B8), 18127–18138.
- Falcon, R.M.S., 1975. Palynostratigraphy of the Lower Karoo sequence in the central Sebungwe District, Mid-Zambezi Basin, Rhodesia. *Palaeontologica Africana* 18, 1–29.
- Falcon, R.M.S., Pinheiro, H., Sheperd, P., 1984. The palynostratigraphy of the major coal seams in the Witbank Basin with lithostratigraphic, chronostratigraphic and palaeoclimatic implications. *Comunicações dos Serviços Geológicos de Portugal* 70, 215–243.
- Fernandes, P., Cogné, N., Chew, D.M., Rodrigues, B., Jorge, R.C.S., Marques, J., Jamal, D., Vasconcelos, L., 2015. The thermal history of Karoo Moatize–Minjova Basin, Tete Province, Mozambique: an integrated vitrinite reflectance and apatite fission track thermochronology study. *Journal of African Earth Sciences* 112, 55–72.
- Foster, C.B., Balme, B.E., Helby, R., 1994. First record of tethyan palynomorphs from the Late Triassic of East Antarctica. *Journal of Australian Geology and Geophysics* 15, 239–246.
- Foster, C.B., Logan, G.A., Summons, R.E., 1998. The Permian–Triassic boundary in Australia: where is it and how is it expressed? *Proceedings of the Royal Society of Victoria* 110, 247–266.
- Galasso, F., Fernandes, P., Montesi, G., Marques, J., Spina, A., Pereira, Z., 2019. Thermal history and basin evolution of the Moatize–Minjova Coal Basin (N'Condédzi sub-basin, Mozambique) constrained by organic maturation levels. *Journal of African Earth Sciences* 153, 219–238. <http://dx.doi.org/10.1016/j.jafrearsci.2019.02.020>.
- Götz, A., Hancox, P.J., Lloyd, A., 2017. Permian climate change recorded in palynomorph assemblages of Mozambique (Moatize Basin, eastern Tete Province). *Acta Paleobotanica* 57 (1), 3–11.
- Götz, A.E., Hancox, P.J., Lloyd, A., 2018. Southwestern Gondwana's Permian climate amelioration recorded in coal-bearing deposits of the Moatize sub-basin (Mozambique). *Palaeoworld*. <http://dx.doi.org/10.1016/j.palwor.2018.08.004> (in press, corrected proof).
- Gobin, N., 1965. Description et répartition des principaux pollenites Permiens, Triasiques et Jurassiques des sondages du bassin de Morondava (Madagascar). *Revue de l'Institut Français du Pétrole* 20 (10), 1415–1461.
- Grantham, G.H., Macey, P.H., Ingram, B.A., Roberts, M.P., Armstrong, R.A., Hokada, T., Shiraishi, K., Jackson, C., Bisnath, A., Manhiça, V., 2008. Terrane correlation between Antarctica, Mozambique and Sri Lanka: comparisons of geochronology, lithology, structure and metamorphism and possible implications for the geology of southern Africa and Antarctica. In: Satish-Kumar, M., Motoyoshi, Y., Osanoi, Y., Hiroi, Y., Shiraishi, K. (Eds.), *Geodynamic Evolution of East Antarctica: a Key to the East-West Gondwana Connection*, 308. Geological Society, London, Special Publication, pp. 91–119.
- GTK Consortium, 2006. Map Explanation. Volume 2: Sheets 1631–1934 Geology of Sheets, Mecumbura, Chioco, Tete, Tambara, Guro, Chemba, Manica, Catandica, Gorongosa, Rotanda, Chimoio and Beira, Mozambique. Ministério dos Recursos Minerais, Direcção Nacional de Geologia, Maputo.
- Hankel, O., 1987. Lithostratigraphic subdivision of the Karoo rocks of the Luwenge Basin (Tanzania) and their biostratigraphic classification based on microfloras, macrofloras, fossil woods and vertebrates. *Geologische Rundschau* 76, 539–565.
- Hankel, O., 1991. Early Triassic plant microfossils from the Kavee Quarry section of the Lower Mariakani Formation, Kenya. *Review of Palaeobotany and Palynology* 68, 127–145.
- Hankel, O., 1992. Late Permian to Early Triassic microfloral assemblages from the Majiya Chumvi Formation, Kenya. *Review of Palaeobotany and Palynology* 72, 129–147.
- Hankel, O., 1993. Early Triassic plant microfossils from Sakamena sediments of the Majunga Basin, Madagascar. *Review of Palaeobotany and Palynology* 77, 213–233.
- Hermann, E., Hochuli, P.A., Bucher, H., Roohi, G., 2012. Uppermost Permian to Middle Triassic palynology of the Salt Range and Surghar Range, Pakistan. *Review of Palaeobotany and Palynology* 169, 61–95.
- Hermann, E., Bucher, H., 2015. Palynostratigraphy at the Permian–Triassic boundary of the Amb section, Salt Range, Pakistan. *Palynology* 39 (1), 1–18.
- Hochuli, P.A., Vigran, J.O., Hermann, E., Bucher, H., 2010. Multiple climatic changes around the Permian–Triassic boundary event revealed by an expanded palynological record from mid-Norway. *Geological Society of America Bulletin* 122, 884–896.
- Jamal, D.L., (Unpublished Ph.D. thesis) 2005. Crustal Studies Across Selected Geotranssects in NE Mozambique: Differentiating Between Mozambican (Kibaran) and Pan-African Events, with Implications for Gondwana Studies. University of Cape Town, Cape Town, South Africa.
- Jha, N., Srivastava, S.C., 1996. Ninth International Gondwana Symposium, Hyderabad. Geological Survey of India Oxford and IBH Publishing Co., New Delhi–Calcutta, pp. 355–368.
- Jha, N., 2006. Permian palynology from India and Africa: a phytogeographical paradigm. *Journal of the Palaeontological Society of India* 51, 43–55.
- Jha, N., Aggarwal, N., Mishra, S., 2018. A review of the palynostratigraphy of Gondwana sediments from the Godavari Graben, India: global comparison and correlation of the Permian–Triassic palynoflora. *Journal of Asian Earth Sciences* 163, 1–21.
- Lächelt, S., 2004. *Geology and Mineral Resources of Mozambique*. Direcção Nacional de Geologia, Maputo.
- Lakshminarayana, G., 2015. Geology of Barcode type coking coal seams, Mecondezi sub-basin, Moatize Coalfield, Mozambique. *International Journal of Coal Geology* 146, 1–13.
- Lindström, S., McLoughlin, S., 2007. Synchronous palynofloristic extinction and recovery after the end-Permian event in the Prince Charles Mountains, Antarctica: implications for palynofloristic turnover across Gondwana. *Review of Palaeobotany and Palynology* 145, 89–122.
- Lopes, G., Pereira, Z., Fernandes, P., Marques, J., 2014. Datação Palinológica dos Sedimentos Glaciogénicos da Formação (Tílica) de Vúzi, sondagem ETA 65, Bacia Carbonífera de Moatize–Minjova, Moçambique–Resultados Preliminares. In: *Actas do IX Congresso Nacional de Geologia 2º Congresso de Geologia dos Países de Língua Portuguesa*, Porto, Portugal, p. 7.
- Msaky, E., Srivastava, V., 1997. Lower Karoo (K5–K6) Palynological assemblage from Tanzania. In: *Abstract 3rd Symposium of African Palynology*. Johannesburg South Africa, p. 31.
- Norconsult Consortium, 2007. Notícia Explicativa: Folhas 1039 Muidine, 1040 Palma, 1134 Ponta Messuli, 1135 Lupilichi, 1136 Milepa, 1137 Macalange, 1138, Negomano, 1139 Mueda, 1140 Mocimboa da Praia, 1234 Metangula, 1235 Macalogue–Chiconono, 1236 Mavago, 1237 Mecula, 1238 Xixano, 1239 Meluco, 1240 Quissanga–Pemba, 1334 Meponda, 1335 Lichinga, 1336 Majune, 1337 Marurupa, 1338 Namuno, 1339 Montepuez, 1340 Mecúfi, 1435 Mandimba, 1436 Cuamba, 1437 Malema, 1438 Ribáuê–Mecubúri, 1535 Insaca, 1536 Gúruê, 1635 Milange e 1636 Lugela–Mocuba, Moçambique. Direcção Nacional de Geologia, Ministério dos Recursos Minerais, Maputo.
- Nyambe, I.A., Utting, J., 1997. Stratigraphy and palynostratigraphy, Karoo Supergroup (Permian and Triassic), mid-Zambesi Valley, southern Zambia. *Journal of African Earth Sciences* 24, 563–583.
- Paulino, F., Vasconcelos, L., Marques, J., 2010. Estratigrafia do Karoo em Moçambique. *Novas Unidades Karoo Stratigraphy in Mozambique*. New Units. In: X Congresso de Geológica dos Países de Língua Portuguesa XVI Semana de Geológica.
- Pereira, Z., Lopes, G., Fernandes, P., Marques, J., 2014. Estudo palinoestratigráfico da sondagem ETA 72 do Karoo Inferior da Bacia de Moatize, Moçambique – Resultados Preliminares. In: *Actas do IX Congresso Nacional de Geologia/2º Congresso de Geologia dos Países de Língua Portuguesa*, Porto, Portugal.
- Pereira, Z., Fernandes, P., Lopes, G., Marques, J., Vasconcelos, L., 2016. The Permian–Triassic transition in the Moatize–Minjova Basin, Karoo Supergroup, Mozambique: a Palynological Perspective. *Review of Palaeobotany and Palynology* 226, 1–19.
- Pereira, Z., Fernandes, P., Lopes, G., Marques, J., Vaz, M., Costa, M., Correia, J., Castro, L., Galasso, F., 2019. Palynology of the Muarádzi sub-basin, Moatize–Minjova Coal Basin, Karoo Supergroup, Mozambique. *Review of Palaeobotany and Palynology* (submt.).
- Pinna, P., Jourde, G., Calvez, J.Y., Mroz, J.P., Marques, J.M., 1993. The Mozambique Belt in northern Mozambique: Neoproterozoic (1100–850 Ma) crustal growth and tectogenesis, and superimposed Pan-African (800–550 Ma) tectonism. *Precambrian Research* 62, 1–59.
- Prasad, B., 1997. Palynology of the subsurface Triassic sediments of Krishna–Godavari Basin, India. *Palaeontographica B* 242, 91–125.
- Retallack, G.J., 1977. Reconstructing Triassic vegetation of eastern Australia: a new approach for the biostratigraphy of Gondwanaland. *Alcheringa* 1, 247–278.
- Riboulleau, A., Spina, A., Vecoli, M., Riquier, L., Quijada, M., Tribouillard, N., Averbuch, O., 2018. Organic matter deposition in the Ghadames Basin (Libya) during the Late Devonian – A multidisciplinary approach. *Palaeogeography, Palaeoclimatology, Palaeoecology* 497, 37–51.
- Riding, J., Warny, S. (Eds.), 2008. *Palynological Techniques* by CA Brown. , second ed. AASP Foundation, The Palynological Society, Dallas, USA.
- Spina, A., Cirilli, S., Utting, J., Jansonius, J., 2015. Palynology of the Permian and Triassic of the Tesero and Bulla sections (Western Dolomites, Italy) and consideration about the enigmatic species *Reduviasporonites chalcatus*. *Review of Palaeobotany and Palynology* 218, 3–14.
- Spina, A., Di Michele, A., Marcogiuseppe, A., Riboulleau, A., Clayton, G., Riquier, L., Vecoli, M., Sassi, P., Rettori, R., Cirilli, S., Servais, T., 2018a. Application of Palynomorph Darkness Index (PDI) to assess the thermal maturity of palynomorphs: a case study from North Africa. *International Journal of Coal Geology* 188, 64–78.
- Spina, A., Stephenson, M.H., Cirilli, S., Aria-Nasab, M., Rettori, R., 2018b. Palynostratigraphy of the Permian Faraghan Formation in the Zagros Basin, southern Iran. *Rivista Italiana di Paleontologia e Stratigrafia* 124 (3), 573–595.
- Srivastava, S.C., Jha, N., 1990. Permian–Triassic palynofloral transition in Godavari Graben, Andhra Pradesh. *Palaeobotanist* 38, 92–97.
- Steiner, M.B., Eshet, Y., Rampino, M.R., Schwindt, D.M., 2003. Fungal abundance spike and the Permian–Triassic boundary in the Karoo Supergroup (South Africa). *Palaeogeography, Palaeoclimatology, Palaeoecology* 194, 405–414.
- Tripaithi, A., Raychowdhuri, A.K., 2005. Triassic palynoflora from the Mahuli–Mahersop Area, Singrauli Coalfield (Southern Extension), Sarguja District, Chhattisgarh, India. *Journal of the Palaeontological Society of India* 50, 77–99.
- Vasconcelos, L., 2013. Coal deposits in Mozambique an overview. In: *Presentation at FFF Mozambique coal conference*, October 2013 – Johannesburg, South Africa.
- Viola, G., Henderson, I.H.C., Bingen, B., Thomas, R.J., Smethurst, M.A., Azevedo, S., 2008. Growth and collapse of a deeply eroded orogen: insights from structural

- and geochronological constraints on the Pan-African evolution of NE Mozambique. *Tectonics* 27, TC5009.
- Ward, P.D., Montgomery, D.R., Smith, R., 2000. Altered river morphology in South Africa related to the Permian-Triassic extinction. *Science* 289, 1740–1743.
- Wood, G.D., Gabriel, A.M., Lawson, J.C., 1996. Palynological techniques-processing and microscopy. In: Jansonius, J., McGregor, D.C. (Eds.), *Palynology: Principles and Applications*, Vol. 1. American Association of Stratigraphic Palynologists Foundation, Salt Lake City, Utah, USA, pp. 29–50.
- Wopfner, H., 1999. The Early Permian deglaciation event between East Africa and northwestern Australia. *Journal of African Earth Sciences* 29 (1), 77–90.
- Wright, R.P., Askin, R.A., 1987. The Permian-Triassic boundary in the Southern Morondava Basin of Madagascar as defined by plant microfossils. In: McKenzie, G.D. (Ed.), *Gondwana Six: Stratigraphy, Sedimentology, and Palaeontology*. Geophysical Monograph, Vol. 41. American Geophysical Union, Washington, DC, pp. 175–197.